

Review

# Research Progress on Singlet Fission in Acenes and Their Derivatives

Jingjing Li <sup>1</sup>, He Cao <sup>1</sup>, Zhibin Zhang <sup>2</sup>, Shuo Liu <sup>1</sup>  and Yuanqin Xia <sup>1,\*</sup><sup>1</sup> Center for Advanced Laser Technology, Hebei University of Technology, Tianjin 300401, China<sup>2</sup> National Key Laboratory of Science and Technology on Tunable Laser, Harbin Institute of Technology, Harbin 150080, China

\* Correspondence: xiayq@hebut.edu.cn

**Abstract:** Solar energy is widely used as a renewable and clean energy, and how to improve the photovoltaic conversion efficiency of solar devices has always been a hot topic. Singlet fission (SF), which converts one singlet exciton into two triplet excitons, is an exciton multiplication generation process in organic semiconductors and is expected to be integrated into solar cells. Moreover, acenes are currently one of the most widely used and popular SF materials. We review recent research on novel acene materials and their developments in the field of solar cells, aiming to provide researchers with ideas for applying the SF process to solar cells.

**Keywords:** singlet fission; acenes; solar cell; photophysics; photochemistry; ultrafast spectroscopy

## 1. Introduction

Today, we face serious environmental pollution problems, such as haze, greenhouse effect, and soil erosion. As such, the development of green and sustainable energy, especially solar energy, is particularly important. There is a wide range of research and most research in this area is conducted on solar energy. Solar cells can efficiently convert solar energy into electrical energy, so how to construct solar devices to achieve high photovoltaic conversion efficiency at low cost is a top priority in research on solar cells [1–8].

The theoretical maximum photovoltaic conversion efficiency of 33% for conventional single-junction silicon solar cells, also known as the Shockley–Queisser (SQ) limit, was calculated by Shockley and his assistant Queisser in 1961 [9]. Much effort has been made in order to break this limit. The multiple exciton generation (MEG) process is regarded as the most promising process to break through this limit, which refers to the absorption of one photon to generate multiple electron–hole pairs [10]. The SF process is one of the most efficient MEG processes. It absorbs one photon and generates two low-energy triplet excitons, each of which can provide an electron for the photocurrent of the photovoltaic device to achieve the effect of current multiplication. Theoretically, the external quantum efficiency of the SF process can exceed 100%, and the photovoltaic conversion efficiency can be increased from 33% of the SQ limit to 44% [11].

The SF process was first discovered in anthracene to explain the delayed luminescence of anthracene [12], and then this phenomenon was found in crystalline tetracene, and increased the fluorescence efficiency of tetracene to 38% [13]. Subsequently, scientists observed the SF phenomenon in pentacene, hexacene, carotenoids, rubrene and some other materials [14–17]. However, because the SF phenomenon could only occur in a few particular materials, and the triplet quantum yield was low, research enthusiasm gradually faded. It was not until 2006 that Nozik proposed that the SF phenomenon had broad prospects for improving the photovoltaic conversion efficiency of solar cells, and the enthusiasm for SF research was rekindled [11]. Subsequently, some new materials were produced, such as acenes and their derivatives, peryleneimides. In 2010, Michl summarized the previous work in the field of the SF process, and proposed a variety of practical



**Citation:** Li, J.; Cao, H.; Zhang, Z.; Liu, S.; Xia, Y. Research Progress on Singlet Fission in Acenes and Their Derivatives. *Photonics* **2022**, *9*, 689. <https://doi.org/10.3390/photonics9100689>

Received: 11 August 2022

Accepted: 21 September 2022

Published: 25 September 2022

**Publisher's Note:** MDPI stays neutral with regard to jurisdictional claims in published maps and institutional affiliations.



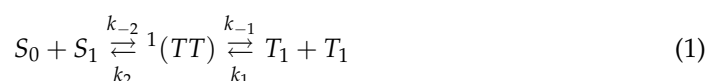
**Copyright:** © 2022 by the authors. Licensee MDPI, Basel, Switzerland. This article is an open access article distributed under the terms and conditions of the Creative Commons Attribution (CC BY) license (<https://creativecommons.org/licenses/by/4.0/>).

chromophores with SF properties that could improve the photovoltaic efficiency of solar cells. They discovered a new type of high-efficiency SF material, 1,3-diphenylisobenzofuran, which laid a foundation for the development of the SF process in the future [18]. In recent years, more complex and efficient SF materials, especially some dimers and trimers, have been prepared through rational design of covalently bound chromophore architectures built with guidance from recent fundamental studies [19,20]. On the one hand, this is in order to explore the mechanism of the SF process, such as the influence of excimers on the SF process, the existence of a charge transfer (CT) state, and the formation and dissociation process of triplet pairs—these issues are still controversial [20–23]. On the other hand, SF materials with a high triplet yield and a long triplet lifetime are prepared for application in photovoltaic devices to enhance their external quantum efficiency [24]. This paper focuses on acene and its derivatives, discusses some new progress in recent years, and summarizes some achievements that have been applied to solar cells.

## 2. Principles and Research Methods of SF

### 2.1. The SF Process

The SF process: An organic chromophore absorbs one photon and transitions to the singlet excited state, this singlet excited state molecule interacts with another adjacent ground state chromophore and transfers partial energy to the ground state chromophore, the two form an coupled triplet state pair  $^1(TT)$ , and the subsequent separation of  $^1(TT)$  produces two free triplet excited states. The simplest description of the SF process that provides insight into the process is shown in Equation (1).



In Equation (1), the interconversion of  $^1(TT)$  with the initial state  $S_0 + S_1$  is described by the rate constants  $k_{-2}$  and  $k_2$ , and the dissociation of the initially formed triplet pair  $^1(TT)$  and  $T_1-T_1$  annihilation are, respectively, described by  $k_{-1}$  and  $k_1$ . In addition, the ratio  $\varepsilon = k_2/k_{-1}$  is often referred to the branching ratio because it reflects the probability of  $^1(TT)$  returning to  $S_1$ . Over time, the SF mechanism has become more complex and controversial, the SF process cannot be described by these rate constants [25].

The mechanism of the SF process has been hotly debated in recent years, and the key to studying it is to understand the process of transition from the singlet exciton state to the intermediate state. Here, we touch upon the mechanism briefly to provide the reader with a background in which to discuss in depth [21,22,25–27]. The simplest description is the one-step direct mechanism (Figure 1a) [25], where the fission rate is determined by direct coupling between  $S_0S_1$  and  $^1(TT)$ . Then, there is the mediated mechanism (or the indirect mechanism), which uses a higher-order perturbation theory, the fission rate is determined by the mixing of  $S_0S_1$  and  $^1(TT)$  with the CT state, which could be real or virtual in nature [25,27]. Specifically, if the off-diagonal diabatic coupling is significant and the energy difference between  $S_1/^1(TT)$  and the CT state is small enough, the transition is mediated by the “virtual” CT state (Figure 1b). When the magnitude of the electronic coupling strength is weak, and there are too high-energy gaps for the CT states, the CT-mediated mechanism becomes negligible and the direct mechanism is dominant [28]. In a different scenario, the CT state may participate directly in the  $^1(TT)$  formation by means of “real” populated intermediates in a two-step mechanism (Figure 1c). However, it is rarely observed and detrimental with the triplet quantum yield [29–31].

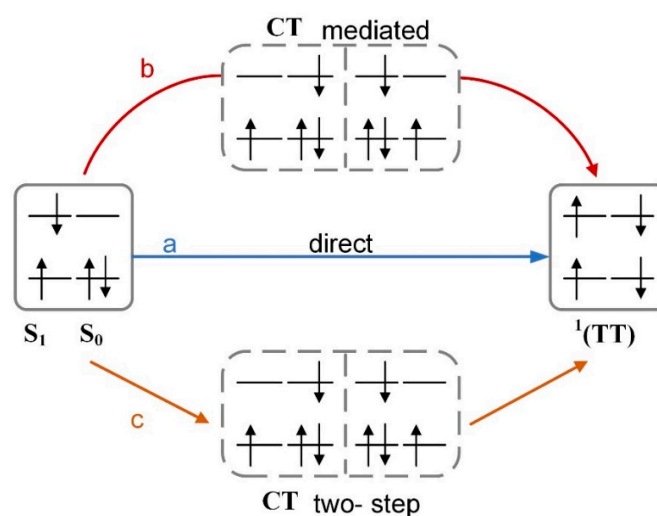


**Figure 1.** (a) Direct, (b) mediated, and (c) two-step mechanism of the SF process.

## 2.2. Condition for SF

The basic requirements of SF materials include strong and broad absorption in the visible light band, a fast fission rate, a high triplet yield and a long triplet lifetime, excellent stability and low cost. At present, two main factors are considered in the development of SF materials: energy matching and coupling.

SF is an ultrafast process, and many other physical processes will compete with it, such as intersystem crossing (ISC) and internal conversion (IC). Therefore, in thermodynamics, in order to ensure that the SF process occupies the dominant position, a certain energy matching relationship needs to be satisfied, and the whole process is preferably exothermic or isothermal. At the same time, the singlet exciton energy is not lower than twice the triplet exciton energy,  $E(S_1) \geq 2E(T_1)$ . Even if this condition is met, the rate of the SF process is not necessarily fast, because triplets may annihilate themselves to form singlets, triplets or quintets. Therefore, it is necessary to satisfy the energy relationship  $E(T_2) \geq 2E(T_1)$ , which can slow the process: triplet excitons annihilate each other to form  $S_0 + T_2$  ( $T_2$  is the next higher-level triplet state) [25]. This is in order to reduce the influence of the  $T_1-T_1$  annihilation process on SF, which can reduce the occurrence of the annihilation process. However, it is not only exothermic systems that can carry out the SF process, the tetracene system is a classic endothermic system. Some studies have found a temperature dependence of the SF process of tetracene (Figure 2) [32]. At 10–140 K, the decay of singlet excitons is accompanied by the increase in triplet excitons, and SF does not change with temperature. This research overturns the statement that the SF process of tetracene is involved in thermal activation. It was also gradually realized that the SF process can also occur in slow endothermic processes in the absence of other competing decay pathways, and additional heat collected by the endothermic SF process can also be used to improve solar cell performance [33–35]. A mechanistic understanding of the endothermic SF process has changed significantly from earliest studies. The energy of  $T_1 + T_1$ ,  $^1(TT)$  is determined by experiments [36], and it was found that  $^1(TT)$  is more stable than  $T_1 + T_1$ , so the initial conditions for the occurrence of the SF process are always allowed, and the endothermic process is mainly concentrated in the second stage  $^1(TT) \rightarrow T_1 + T_1$ , it is related to the energy transfer of the triplet state or molecular packing [34,37]. The studies on the properties of  $^1(TT)$ , including dynamic equilibrium with  $S_1$  [38], ultrafast formation in a strongly exothermic system [39], and theoretical re-evaluations of triplet-pair interactions [21,40], have highlighted the current debate about the nature of  $^1(TT)$ .

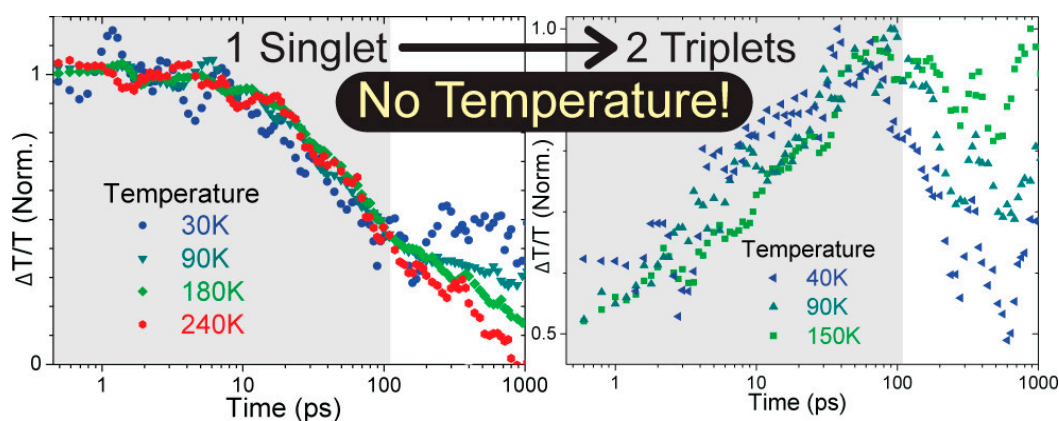


**Figure 2.** The temperature-dependent dynamics of the TA signal for singlet and triplet excitons in a tetracene film. Reprinted with permission from Ref. [32]. Copyright 2013, American Chemical Society.

If energy matching is a prerequisite for the occurrence of the SF process, the coupling between chromophores is the key factor for the occurrence of the effective SF process. Taking tetracene as an example, it does not meet the strict energy conditions. The SF process is an endothermic process, but its triplet quantum yield in the crystalline state is very high, we believe that this is closely related to the coupling between chromophores in the crystalline state. The tetracene polycrystalline film obtained by thermal evaporation has a faster SF rate than the tetracene crystal grown by solution, because the thermal evaporation of the tetracene polycrystalline film has high order and fewer defects [41]. There are two crystal structures of 1,3-diphenylisobenzofuran, and only the polycrystalline film with  $\alpha$  morphology exhibits an efficient SF process, resulting in a triplet exciton yield of 200% at 77 K and 140% at room temperature. Because two molecular interactions between the molecular pillars of the slip stacking layers are different in the crystal form, resulting in a much smaller triplet quantum yield in the  $\beta$  morphology crystal [42]. The substituents of the diphenyl-substituted tetracene limit the growth of crystals, and molecules are arranged in a disordered manner, resulting in the formation of noncrystalline amorphous films, but it exhibits surprisingly high SF yields in a few hundred picoseconds, and it produces triplet quantum yields as high as 122% [43]. In other words, different states of molecules have different molecular orientations and intermolecular interactions, resulting in different efficiencies of the SF process. Through theoretical calculations and experiments, it was concluded that the coupling between chromophores cannot be too weak or too strong. If the coupling is too weak, it will be unfavorable for the SF process to compete with other physical processes, and  $^1(TT)$  cannot be effectively formed, which causes exciton-exciton annihilation and reduces the SF efficiency. Physical contacts between molecules in crystals or aggregates, and covalent linkages in dimers or polymers, are all beneficial for the coupling between chromophores, which provides theoretical support for designing more efficient SF materials and improving the SF process rate.

### 2.3. Experimental Method

Various techniques have been applied in detection of the SF process due to the fast development of laser technology. This section will focus on two commonly used experimental methods, transient absorption (TA) spectra and time-resolved fluorescence spectra, due to their advantages in measuring dynamics of materials.

**Transient absorption spectra.** The SF process generally occurs on the time scale of ultrafast, so that time-resolved TA spectra is essential to study its physical process [44–49]. Depending on the time scale, TA spectra is generally divided into fs TA and ns TA spectra. The TA spectra is based on the pump–probe technique and involves two beams of light. For fs TA spectra, usually femtosecond pulse passes through a nonlinear medium to

generate white light continuum as probe pulse, and the other beam passes through an optical parametric amplifier to generate wavelength-tunable pump pulse. A fraction of the molecules is excited by a pump pulse, then a probe pulse is sent through the sample by a mechanical delay. In addition to the pulse width of the pump pulse is different from fs TA spectra, the probe pulse of ns TA spectra is usually a light source produced by an inert gas, which can generate a pulse of the order of ms and has a very wide spectral range. In addition, the time delay in ns TA spectra is controlled by electrical delay, which is also different from fs TA spectra. A difference absorption spectrum is calculated at different time delays, the absorption spectrum of the excited sample minus the absorption spectrum of the sample in the ground state ( $\Delta A$ ) [50]. The spectrum  $\Delta A$  contains contribution from the ground-state bleach (GSB), stimulated emission (SE) and excited-state absorption (ESA). When the sample is excited, different components, such as singlet excitons, triplet excitons, and coupled triplet pairs, will correspond to different absorption peaks. Analyzing the TA data at different delay times can obtain the information on the growth or decay of different components and information such as the rate of the SF process. If the absorption peaks are close and overlap, the dynamics of different components can also be understood by means of global target analysis, and singular value decomposition.

**Time-resolved fluorescence spectra.** Time-resolved fluorescence spectra focus on fluorescence, unlike TA spectra which tracks both the bright and dark state species created upon excitation. It detects the change in fluorescence over time after excitation, which reflects more information about the dynamics of the lowest excited state [51–53]. Furthermore, different methods are selected depends on the chosen time window for lifetime measurement. Time-correlated single-photon counting (TCSPC) is a unique time-resolved fluorescence measurement method that collects fluorescence by a single photon and measures the excited state fluorescence lifetime on a time scale of nanoseconds to microseconds [49,52,54]. Fluorescence up-conversion (FUC) technology measures fluorescence lifetime on ultra-fast time scales from femtoseconds to nanoseconds. Some electronic processes, such as energy transfer, excitation delocalization, all take place in this time scale, so FUC is very suitable to understand their dynamics [49,55]. For an exponentially fitted decay profile, the fluorescence lifetime is the time it takes for 63% ( $1-1/e$ ) of the population of the excited electrons to return to the ground state. Lifetime measurement can help us better understand the energy transfer, triplet state generation process and other information that occur in organic molecules. To study general SF process comprehensively, both TA spectra and time-resolved fluorescence spectra are needed most of the time.

### 3. SF Materials

In order to achieve high photovoltaic conversion efficiency of photovoltaic devices, it is necessary to select and study suitable SF materials. At present, there are many materials which can occur in the SF process, but scientists still lack an understanding of the factors which promote the SF process. There are a few SF materials whose triplet exciton yield can reach 200%, such as tetracene [56], pentacene [57], hexacene [58,59], 1,3-diphenylisobenzofuran [42,60]. Some studies found that the SF efficiency of single-crystal pentacene was higher than that of its vacuum deposition film, because the film mainly existed in the form of excimer after being excited, and the SF yield was only 2% [61–63]. In addition, the SF process was also found in covalently linked dimer of tetracene, and the efficiency was lower than that of tetracene crystal [64–66]. Molecular structure, intermolecular arrangement and crystal packing can all affect the SF process [67,68]. This section introduces some recent studied acene monomers and their oligomeric, and their SF process has been found in systems such as noncrystalline solid film, nanoparticle and solution [43,69,70]. Tables 1 and 2 summarize the time scales of SF in monomers and dimers.

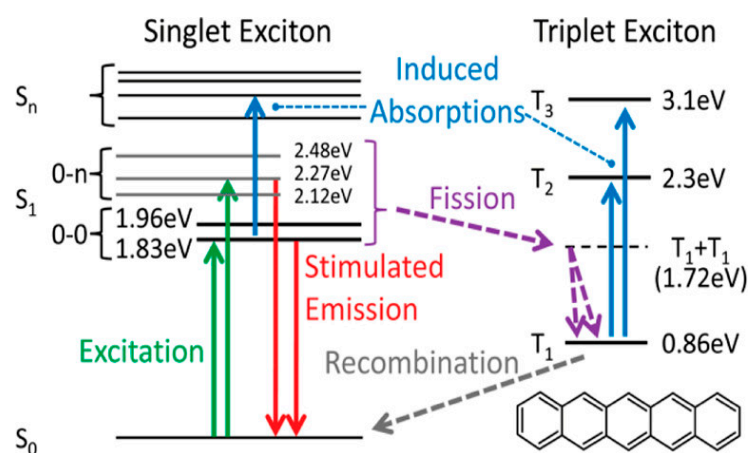
#### 3.1. Monomer

**Tetracene.** Linear acenes are the most widely studied and typical SF materials. A large number of theoretical studies and experimental data on tetracene, pentacene and their

derivatives show that they can perform the SF process quickly and efficiently. The singlet excited state energy of tetracene is approximately equal to twice the triplet excited state energy, its SF process is a slightly endothermic process and occurs in the range of 10–100 ps. Some studies believe that the singlet exciton state  $S_1$  and the multi-exciton intermediate state ME are coherently superimposed to form a higher-energy ME state [56]. The entropy increase in the tetracene crystal acts as the driving force to decay the  $S_1 \leftrightarrow$  ME superposition state into two triplet excitons, resulting in a higher SF rate and a temperature-independent fission rate in the tetracene crystal. However, through experiments, Wilson found that in the temperature range of 10–270 K, the initial decay process of tetracene singlet excitons (within 200 ps) had no temperature dependence, and its SF process did not change with temperature, but the process after the initial decay (over 200 ps) showed a clear temperature dependence [32].

**Tetracene derivatives.** For two tetracene derivatives with PEG groups of different lengths (PhTc-PEG-1 with a short PEG chain and PhTc-PEG-2 with a long PEG chain), the SF process can be conducted in these two nanoparticles via a real charge-transfer (CT) intermediate state. However, the formation of the real CT state is not conducive to the occurrence of the SF process, resulting in relatively low SF yields for two nanoparticles (60.6% and 53.3% for PhTc-PEG-1 and PhTc-PEG-2). The PhTc-PEG-2 nanoparticle has a lower SF yield because of the weaker interaction, so that the long PEG chain should be avoided when modifying SF chromophore [71]. In addition to modifying the chain length of the chromophore, the introduction of different functional groups also has an effect on the SF rate, for example, the hydrophilic effect of carboxyl groups. Compared with PhTc, PhTc-COOH molecules are more parallel and tighter in the nanoparticles, which enables stronger coupling between adjacent tetracene, enabling faster and more efficient SF process [72].

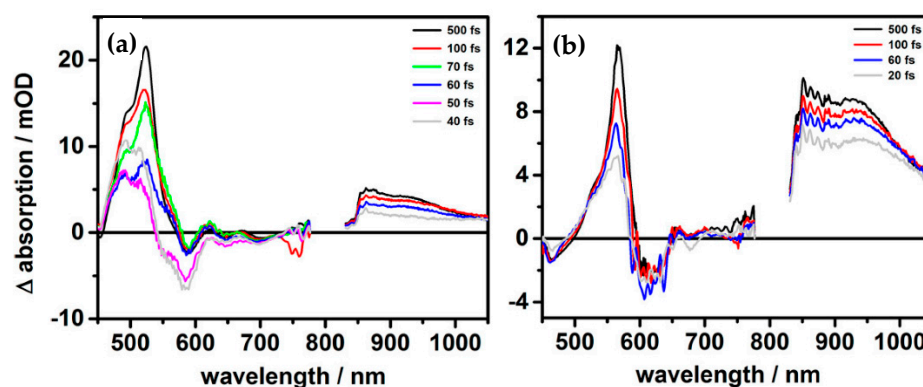
**Pentacene.** Different from tetracene, pentacene is a ‘star’ molecule in electronics, and its SF process is an exothermic system. The previous studies are less about pentacene, because the pentacene molecule basically does not glow, and the internal process is too fast. It was not until the appearance of pump–probe technology that scientists slowly began to understand and clearly observe the SF process of pentacene. From the partial Jablonski diagram of pentacene (Figure 3), it can be seen that its lowest singlet excited state energy is 1.83 eV, which is approximately 100 meV higher than the twice energy of the triplet excited state (0.86 eV) [44,73]. Moreover, because of the strong intermolecular coupling of pentacene crystal, pentacene’s SF process occurs in ultrafast time scale of 80–110 fs and it is a unidirectional and exothermic process. From then on, the research on pentacene is not limited to crystals, but also amorphous film [69], solution [52,57], its related derivatives [74].



**Figure 3.** Partial Jablonski diagram of crystalline pentacene. Reprinted with permission from Ref. [73]. Copyright 2013, American Chemical Society.

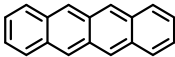
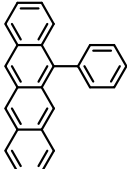
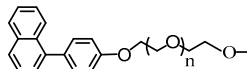
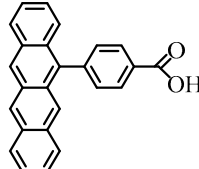
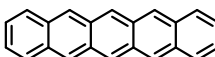
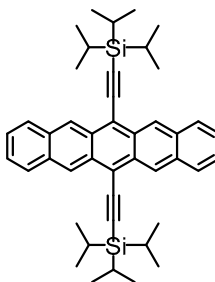
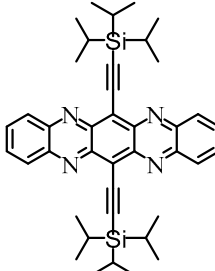
**Pentacene derivatives.** Due to the unsubstituted acene molecules have relatively low solubility and poor photostability, the acene derivatives substituted with different functional groups have been designed. The conjugated alkyl chains are introduced at the 6, 13 positions of pentacene to obtain a pentacene modified by triisopropylsilylethynyl, which improves the solubility and air stability of the pentacene molecule [74]. The SF mechanism of TIPSpentacene in concentrated solution is dominated by diffusive encounters, and has a long free triplet state lifetime (6.5  $\mu$ s) and a high triplet yield ( $\sim$ 200%). The above results indicate that TTA is suppressed in concentrated solutions [57]. However, in dilute solution, due to the too large intermolecular distance, the diffusing molecules cannot combine during the lifetime, and the SF process cannot be efficiently generated. Walker found in concentrated solutions of TIPSpentacene that a transient bound excimer intermediate was formed by the collision of one photoexcited and one ground-state TIPS–pentacene molecule, and the intermediate broke up when the two triplets separated to each TIPS–pentacene molecule. Dvorak did not find the existence of excimers in the experiment, which was in sharp contrast to the findings of Walker [52]. Dvorak believed that the SF process occurred mainly through diffusive encounters, and denied the statement of Grieco [75] that the SF process did not occur through diffusive encounters. In addition, Grieco also found a nonlinear relationship between SF rate and concentration, which was attributed to molecular crowding effects.

For the TIPSpentacene film, many experiments have shown that its singlet excited state  $S_1$  and ME state coexist. The  $S_1$  and ME excitons undergo the decoupling of ME from  $S_1$ , and evolve into the state of ME' state over the course of  $\sim$ 200 fs. Subsequently, the ME' state decays to the  $T_1$  state with a time constant of  $\sim$ 1.5 ps [76]. Herz added  $sp^2$  nitrogen atoms to the backbone of TIPS–pentacene, which led to the evolution of  $S_1$  and ME to ME' state over the course of 110 fs and doubled the rate of the SF process (Figure 4). This result underlines the potential of aza derivatives to optimize efficiencies by eliminating loss channels. Moreover, comparing with TIPS–pentacene, Diaza–TIPS–pentacene has a stronger  $T_1 \rightarrow T_n$  signal in the near-infrared spectrum, which may lead to the higher triplet quantum yield of Diaza–TIPS–pentacene [77].



**Figure 4.** Transient absorption spectra at several probe delay times for (a) TIPS–Pn and (b) Diaza–TIPS–Pn. Reprinted with permission from Ref. [77]. Copyright 2014, American Chemical Society.

**Table 1.** Summary of time scales of the SF process in monomers.

Monomer	Structure	Name	S <sub>1</sub> Decay Time	Intermediate State Lifetime	TT Lifetime	T <sub>1</sub> Lifetime	SF Yield	Reference
		Tetracene			—		~200%	[56]
Tetracene and its derivatives		PhTc	1.9 ps	49.5 ps (*S <sub>1</sub> )	797.0 ps	11.3 ns	67 ± 15%	[72]
		PhTc-PEG-1 (n = 1)	1.94 ps	409.14 ps (CT)	—	14.62 ns	60.6%	[71]
		PhTc-PEG-2 (n = 4)	2.69 ps	566.63 ps (CT)	—	19.61 ns	53.3%	
		PhTc-COOH	17.2 ps	—	229.9ps	34.7 ns	133 ± 10%	[72]
		Pentacene	~80 fs		—		160–180%	[44]
Pentacene and its derivatives		TIPS-pentacene	200 fs	1.2 ps (S <sub>1</sub> /ME)	—	>1 ns	144%	[77]
		Diaza-TIPS-pentacene	110 fs	1.0 ps (S <sub>1</sub> /ME)	—	>1 ns	—	[77]

### 3.2. Dimers

Acene dimers are most common dimer that perform the SF process. Two chromophores that can generate the SF process are connected by covalent bonds to form dimers, such as tetracene dimers, pentacene dimers [78–80]. Most chromophores typically exist in solid-state crystals; however, when these molecules are covalently coupled, dimers can serve as model systems to study fundamental photophysical dynamics. This part describes several factors that affect SF rates and triplet yields in dimers, such as through-space coupling, through-bond coupling and connecting bridge. Some of the material structures mentioned are shown in Figure 5.

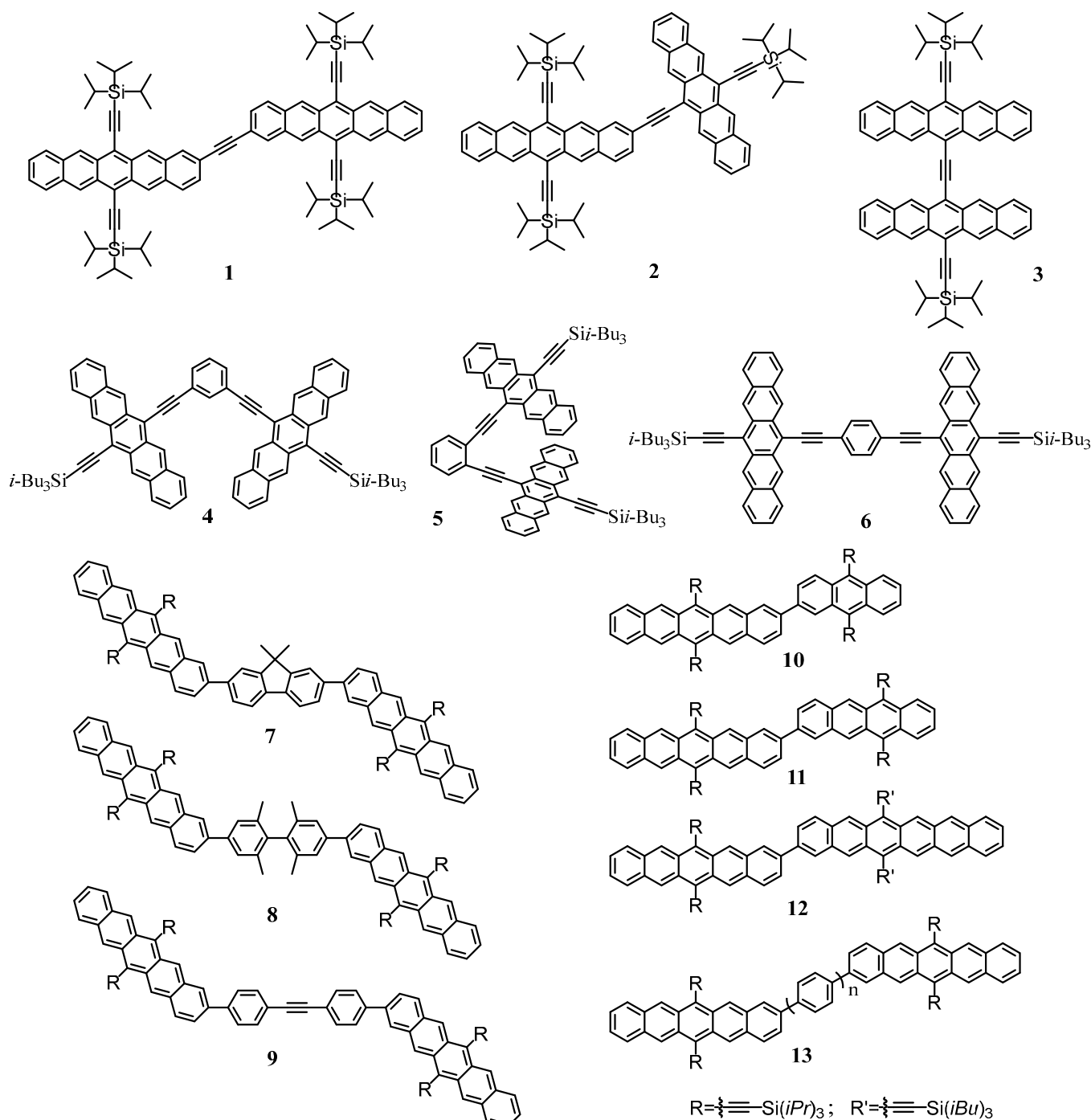


**Figure 5.** Structures of partial pentacene dimers considered in this review.

**Through-space coupling.** The main factor affecting the SF rate and the triplet yield of the dimer is the electronic coupling of the two chromophores, which is not only affected by through-bond coupling between the chromophores, but also has a close relationship with their relative positions [81]. Korovina synthesized two tetracene dimers: BET-X with a large overlap of tetracene  $\pi$  orbitals, and BET-B with less overlap between the tetracene  $\pi$  orbitals because of twisted arrangement. The former has a faster intramolecular singlet fission (iSF) rate than the latter, which shows the dominance of the spatial coupling [64]. Sumitha obtained pentacene dimers (Figure 5 1–3) of three different configurations with slip-stacked (2,2' BP, J-type), oblique (2,6' BP), facial (6,6' BP, H-type) by covalently linking pentacene with an acetylene bridge at different positions and their fs TA spectra (Figure 6) [79].

In the 2,2' BP with slip-stacked configuration, through-space coupling dominates, and the iSF efficiency reaches 182%. In the 2,6' BP with oblique configuration, the degree of chromophore overlap becomes smaller, the through-space coupling becomes weaker, and the iSF efficiency dropped to 97%. At 6,6' BP, facial configuration, strong electronic coupling leads to the formation of excimers. These excimers prevent the formation of correlated triplet pairs, which in turn hinders the efficient iSF process.

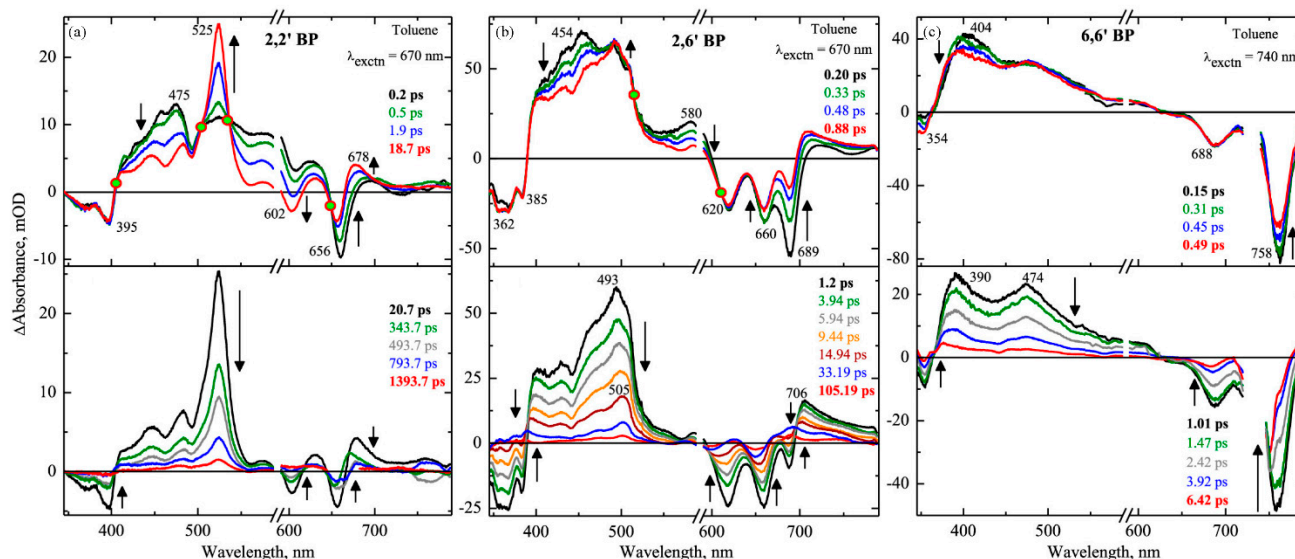


**Figure 6.** Femtosecond transient absorption spectra of (a) 2,2' BP, (b) 2,6' BP, and (c) 6,6' BP in toluene obtained upon excitation at different delay times. Reprinted with permission from Ref. [79]. Copyright 2022, American Chemical Society.

**Table 2.** Summary of time scales of the SF process in dimers.

Dimers	Name	Solvent	SF Time Scale	TT Lifetime	Triplet Yield	References
Tetracene dimers	BET-B	THF	$2 \pm 0.5$ ps	—	$154 \pm 10\%$ (film)	[64]
	BET-X	toluene	<180 fs	—	—	
	2,2' BP	toluene	$13.45 \pm 0.5$ ps	$495.41 \pm 15$ ps	182%	[79]
	2,6' BP	toluene	$5.85 \pm 0.25$ ps	$17.29 \pm 0.8$ ps	97%	
	6,6' BP	toluene	$2.26 \pm 0.25$ ps	—	—	
Pentacene dimers	m-2	benzonitrile	$63.0 \pm 6.3$ ps	$2.2 \pm 0.1$ ns	$156 \pm 5\%$	[82]
		THF	$70.3 \pm 7.0$ ps	$2.5 \pm 1.0$ ns	$132 \pm 2\%$	
		toluene	$90.2 \pm 9.0$ ps	$2.6 \pm 0.1$ ns	$125 \pm 5\%$	
	o-2	benzonitrile	$0.5 \pm 0.2$ ps	$12.0 \pm 0.3$ ps	—	
		toluene	—	—	—	
	p-2	benzonitrile	$2.7 \pm 1.0$ ps	$17.3 \pm 1.3$ ps	$130 \pm 10\%$	
		toluene	—	—	—	
	BP0	chloroform	760 fs	0.45 ns	~200%	[78]
	BP1	chloroform	20 ps	16.5 ns	~200%	
	BP2	chloroform	220 ps	270 ns	~200%	
	FL-PD	toluene	$7.14 \pm 0.3$ ps	$186.67 \pm 4.5$ ps	$197.8 \pm 5\%$	[83]
	MBP-PD	toluene	—	~147.05 ns	$16 \pm 2\%$	
	DPA-PD	toluene	$10.71 \pm 0.5$ ps	$1.09 \pm 0.05$ ns	$185.12 \pm 6\%$	
Heterodimers	PA	chloroform	(S <sub>1</sub> lifetime = 11.5 ns)	—	—	[84]
	PT	chloroform	0.83 ps	2.4 ns	—	
	PH	chloroform	1.2 ps	0.21 ns	—	

**Through-bond coupling.** Pentacene dimers are linked via a phenylene spacer in an ortho-, meta- and para-arrangement (Figure 5 4–6) exhibit different iSF efficiencies in solution. In the ortho-isomer, through-space coupling should dominate due to the unique spatial proximity of the pentacenes. On the contrary, the electronic coupling element, which governs SF and TTA process, is mediated through-bond in the meta- and para-isomers, and the meta-isomer reaches a triplet quantum yield as high as  $156 \pm 5\%$  [82].

The above materials adjust the coupling strength between chromophores through the substitution of molecular spacers at different positions, so as to achieve the purpose of regulating SF efficiency. In addition, it can also be adjusted by changing the length of molecular spacer. The dimer is obtained by para-linking of triisopropylsilylethynyl-modified pentacene through phenylene (Figure 5 13), and the length of the spacer is variable [78]. This linking makes the through-bond coupling between two chromophores dominant and avoids the influence of spatial coupling. With the increase in spacer, it was found that the lifetime of triplet pair is extended from 0.5 to 270 ns, because the distance between the two triplet chromophores in the molecule increases, the coupling effect weakens, and the rate of TTA decreases.

The planarity and length of the bridges in the pentacene dimer also affect the efficiency of the SF process. Paul synthesized different pentacene dimers: FL-PD, DPA-PD (which had planar structures), and MBP-PD (which possessed a twisted bridge) (Figure 5 7–9) [83]. Through their femtosecond TA spectra (Figure 7a–c), it was found that FL-PD have a faster iSF rate (187 ps) and exhibit higher efficiency (198%), compared to MBP-PD which shows a low efficiency of  $\sim 16\%$ . However, the DPA-PD with a longer bridge length shows a slower iSF process (1.09 ns), compared to FL-PD, and the efficiency reaches 185%. From this, it can be inferred that the flatness of the pentacene dimer bridge should be maintained and the distorted structure should be avoided when designing efficient SF materials for photovoltaic devices.

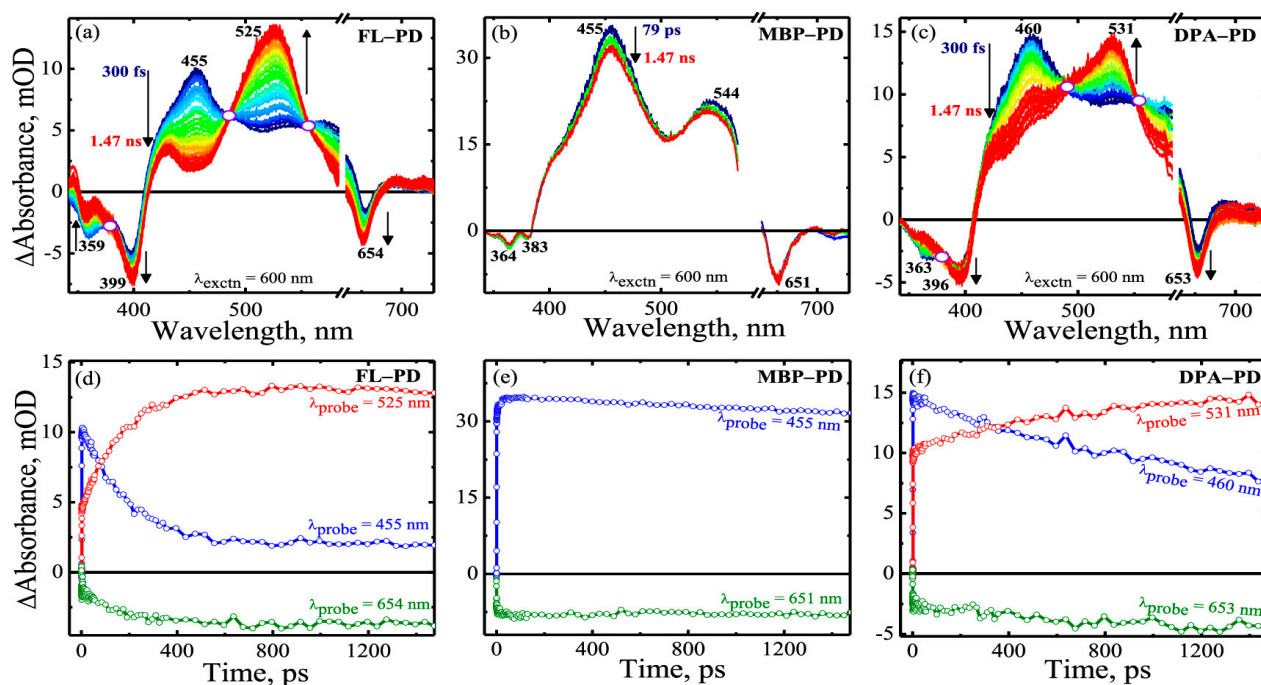


**Figure 7.** Femtosecond transient absorption spectra of (a) FL-PD, (b) MBP-PD, and (c) DPA-PD in toluene obtained upon excitation at 600 nm. The delay times are given and the arrows show the spectral evolution. Kinetic profiles of (d) FL-PD, (e) MBP-PD, and (f) DPA-PD probed at the maximum of singlet, triplet state absorption, and ground-state bleach are given. Reprinted with permission from Ref. [83]. Copyright 2021, American Chemical Society.

**Chromophore influence.** The dimer formed by the same type of chromophore can basically meet the requirements of energy matching, and its SF efficiency mainly depends on the electronic coupling between the chromophores. However, if it is a heterodimer formed by different types of chromophores, whether the SF process can occur, the energy matching relationship must first be considered. The SF process is different when the TIPS-modified pentacene is linked with TIPS-modified anthracene, tetracene or hexacene through covalent bonds to form oligoacene heterodimers (Figure 5 10–12 [84]). The energy of the associated triplet exciton pair of the heterodimer is the sum of the energies of the two monomers, while the energy of the singlet state is determined by the lower-energy chromophore. Therefore, in theory, the dimer formed by pentacene and anthracene cannot occur SF phenomenon, and the experimental results also prove this point. In these heterodimeric systems, the formation of related triplet pairs is not affected by the driving force, and the SF-related mechanism remains to be further revealed.

### 3.3. Trimers and Tetramers

The pentacene dimer exhibits a high iSF rate in both solution and thin film. In contrast, it is difficult for tetracene to achieve an efficient iSF process. The higher the rate of the iSF process and triplet yields were displayed in a linear tetracene trimer, compared with its dimers, indicating that exciton delocalization was an important factor driving the SF process [53]. However, the triplet quantum yield of the tetracene trimer (~96%) is smaller than that of the pentacene dimer (~200%). To improve the iSF efficiency of tetracene compounds, Li synthesized a novel covalently linked tetracene tetramer (Figure 8 1) [85]. Compared with the trimer, the triplet quantum yield of the tetracene tetramer is significantly increased (128%) and the lifetime of most free triplet excitons exceeds 100  $\mu$ s. This is the first time that a triplet quantum yield of more than 100% has been obtained in solution of tetracene compounds. Sakai first synthesized a cyclic pentacene trimer with a tubular conformation, with a cylindrical hollow cavity of 1.5 nanometer in length and a sub-nanopore. The nanotubes undergo space-type iSF via effective intramolecular interactions, with up to 180% triplet quantum yield and long free triplet state lifetime (80  $\mu$ s) [86].

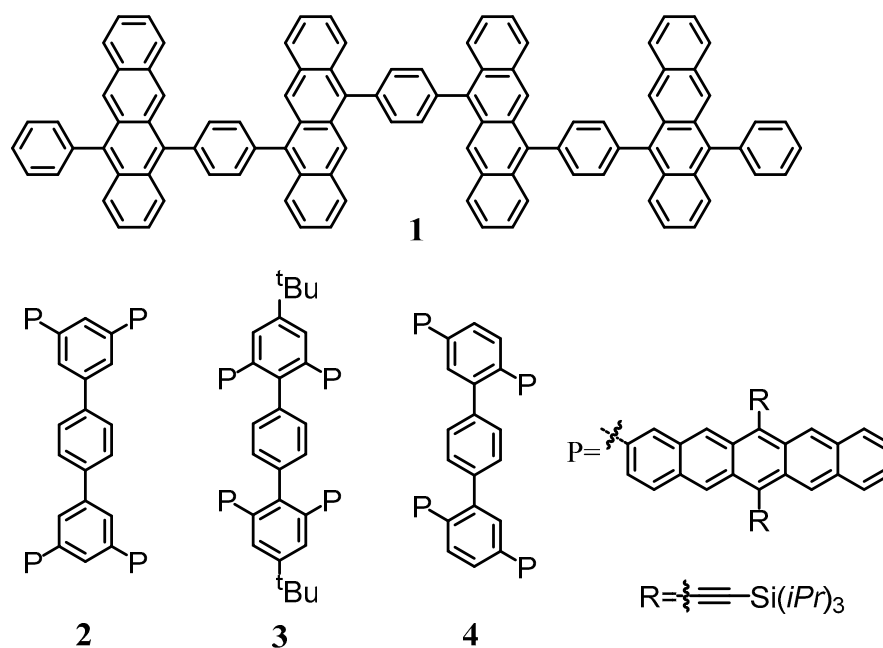


**Figure 8.** Structures of partial tetramers considered in the review.

Xia designed three different terphenyl-bridged TIPS-pentacene tetramers (Figure 8 2–4). Changing the bonding position of the TIPS-pentacene chromophore along the triphenyl ring can control the degree of steric hindrance within individual tetramer, which in turn

can determine the degree of intermolecular coupling in the solid state [87]. If the coupling between the chromophores of the tetramer is strong, the fast iSF process can occur in the case of weak intermolecular coupling. The rapid occurrence and slow decay of the iSF process can be controlled with adjusting the degree of molecular steric hindrance, high yield and long life of triplet state can be obtained (Figure 9). Different geometries of molecules have different effective triplet transport efficiencies. How to control local molecular packing to combine iSF and intermolecular SF (xSF) process to maintain a fast formation rate of triplets and achieve high quantum transfer efficiency, are important for future exploration about the design of device structures.

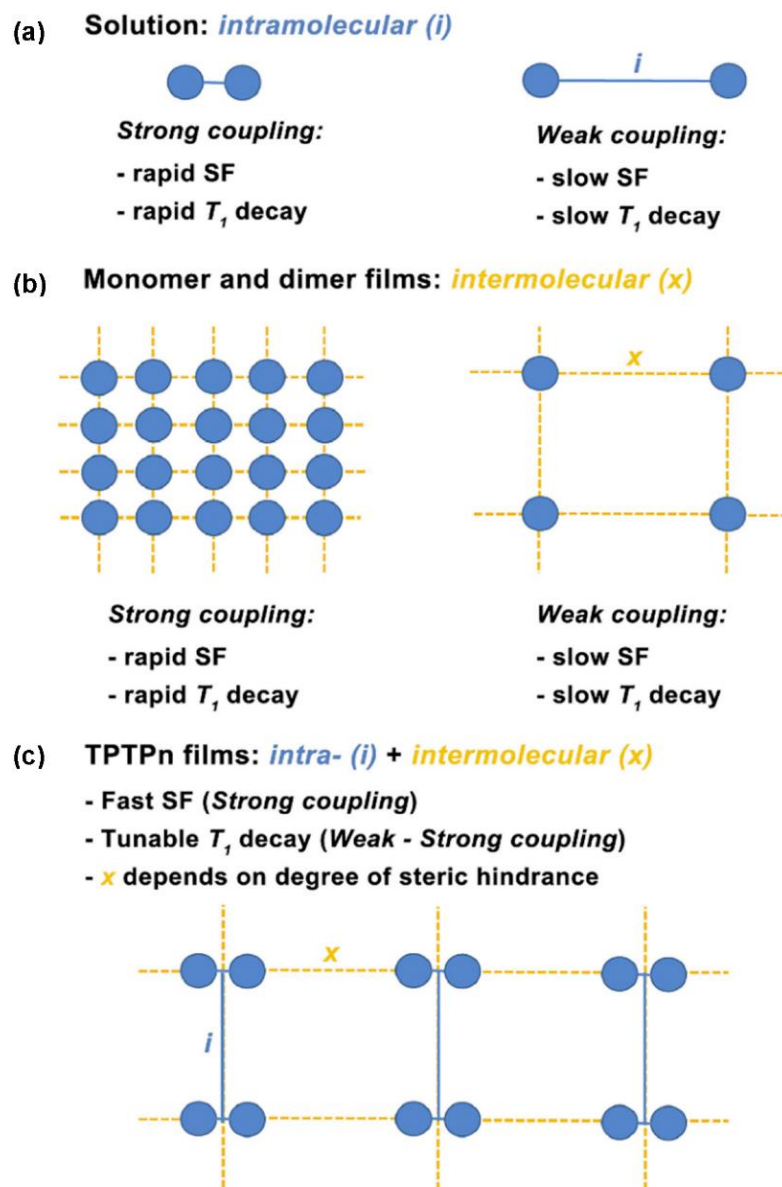


**Figure 9.** Summary of structure–function relations and the design strategy based on TPTPn compounds. Solid blue lines correspond to through-bond interactions, and dashed orange lines denote through-space interactions. (a) Typical solution-phase intramolecular SF dynamics. (b) Film dynamics for monomer and dimer materials. (c) The design strategy based on TPTPn compounds. Reprinted with permission from Ref. [87]. Copyright 2019, Elsevier Inc.

In summary, acenes and their derivatives are ideal SF materials. Although scientists have made many progress in their research, there are still some shortcomings. For example, the mechanism of SF occurrence in different types is still unclear. It is clear that if we can

further understand the occurrence mechanism, it will be of great help to design acene and its derivative materials and put them into practical application in the future.

#### 4. Device Applications

In theory, an organic molecule can absorb a photon and convert it into two triplet excitons through the SF process, but this is only the first step in completing the photovoltaic conversion. Applying SF materials to construct photovoltaic devices that excitons can become free charges and complete the conversion from light energy to electrical energy is the fundamental driving force for the research and development of the SF process. This section describes the application of acene materials in photovoltaic devices, including organic photovoltaic devices and inorganic solar cells.

##### 4.1. Organic Photovoltaic Devices

Pentacene is first put into practical applications due to its ultrafast fission properties. Lee constructed a pentacene/ $C_{60}$  heterojunction organic multilayer photodetector. The experiment measures an exciton multiplication factor of  $145 \pm 7\%$ , and it proves that the quantum efficiency of organic photodetectors can be improved by utilizing the SF process in pentacene [88]. Congreve introduced a poly (3-hexylthiophene) exciton confinement layer in a conventional pentacene/ $C_{60}$  heterojunction device and placed it between the pentacene and the anode. This structure increases the external quantum efficiency of the device to 109% for the first time [89]. Thompson then exploited a distributed Bragg reflector (Figure 10) to make the external quantum efficiency of this kind of device increase to 126% [90].

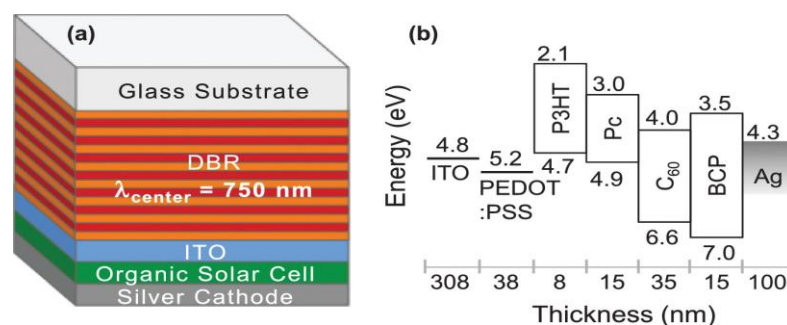


**Figure 10.** (a) Schematic diagram of distributed Bragg reflector light management system and organic solar cell and (b) device structure and energy levels of the pentacene solar cell with device thicknesses in nanometers. Reprinted with permission from Ref. [90]. Copyright 2013, AIP Publishing.

The thicker the pentacene film in the layered battery, the more photons are absorbed, but the distance of excitons diffusing to the boundary also increases, which hinders the separation of charges. Rao detected pentacene/ $C_{60}$  heterojunction (Figure 11) with no emission within 200 fs by using transient spectra and the formation of the charge was approximately 2–10 ns [91]. Chan observed a much faster charge generation process using time-resolved two-photon photoemission (TR-2PPE) spectra techniques [92]. Chan uses an almost monolayer of pentacene film, the thickness of the pentacene film used by Rao is approximately 150 nm, which makes the triplet excitons to diffuse slowly. So it can be seen that the film thickness has a great influence on the physical process in the device.

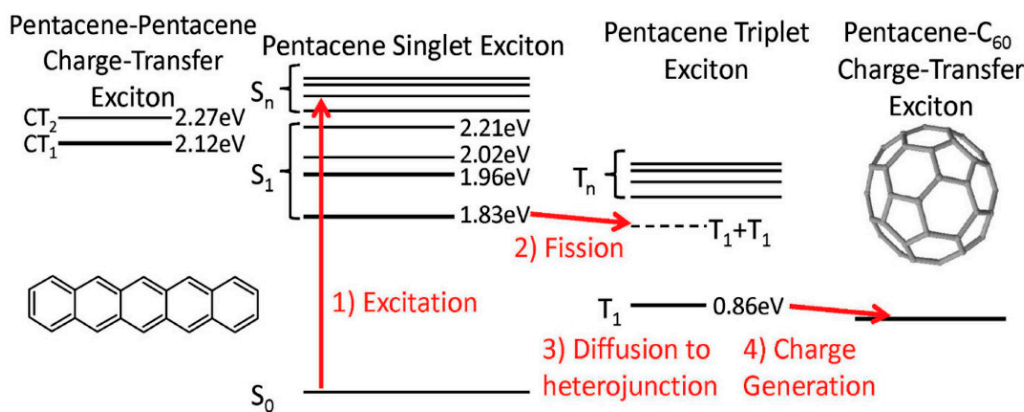


**Figure 11.** Molecular structures of pentacene and C<sub>60</sub> and an energy level diagram for excitonic states in pentacene. Reprinted with permission from Ref. [91]. Copyright 2010, American Chemical Society.

To achieve high solar energy conversion efficiency, the ionization interface of the triplet state should be composed of pentacene and a material with strong infrared absorption. Wilson used the special pairing of pentacene and PbSe quantum dots to produce a device with a power conversion efficiency as high as 4.7% (Figure 12), while the energy conversion was only 1% after switching to PbS [73]. This is because PbSe has a lower ionization potential, which is favorable for the separation of triplet excitons than PbS. Jadhav randomly combined SF donors (such as pentacene, 6,13-diphenyl-pentacene) and acceptors (such as fullerenes, perylene diimides, PbS and PbSe nanocrystals) to investigate triplet dissociation processes at different energy levels [93]. It has been found experimentally that exciton dissociation in heterojunctions is very sensitive to changes in the energy level structure of the donor and acceptor, so it is important to select a suitable acceptor to meet the requirements of efficient separation of triplet excitons in SF solar cells.

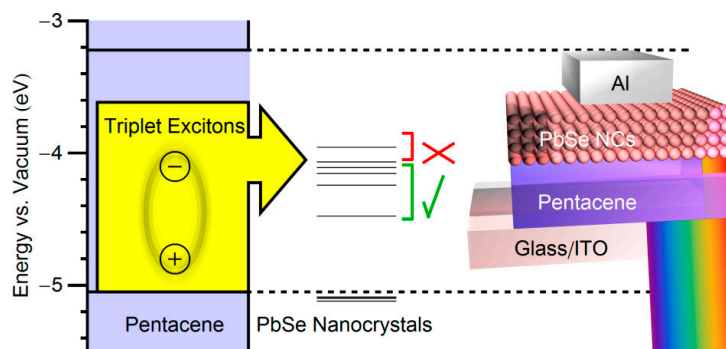


**Figure 12.** Illustration of the use of a size series of quantum dots with varying bandgaps to establish a lower limit on the energy of the ionizing exciton, and a schematic diagram of a pentacene/nanocrystal hybrid solar cell. Reprinted with permission from Ref. [73]. Copyright 2013, American Chemical Society.

Pure pentacene has poor photostability, many studies have designed functionalized pentacene to form a bilayer solar cell with other materials. Ehrler constructed a bilayer heterojunction architecture between TIPS–pentacene and PbSe and PbS nanocrystals, respectively (Figure 13). These TIPS–pentacene devices show promising power conversion efficiencies of more than 4.8% [94]. It is the first solution-processable SF system, and in the TIPS–pentacene absorption range, the external quantum efficiency is as high as 60% and the internal quantum efficiency reaches 170%.

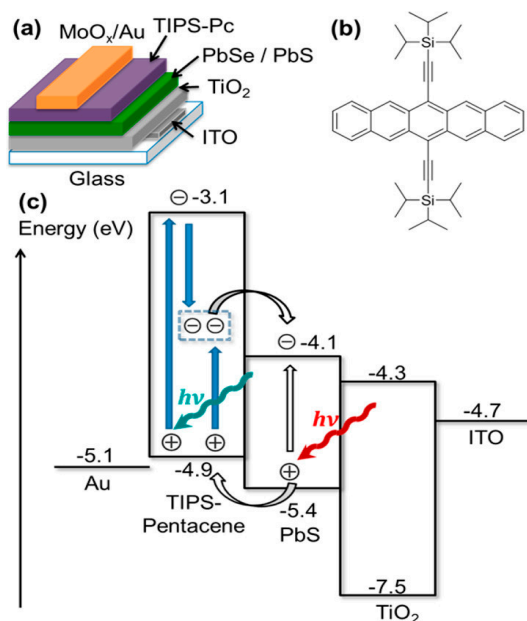


**Figure 13.** (a) Device architecture of the nanocrystal/TIPS-pentacene photovoltaic device. (b) Chemical structure of TIPS-pentacene. (c) Alignment of energy levels in the PbS/TIPS-pentacene device. Reprinted with permission from Ref. [94]. Copyright 2015, American Chemical Society.

Tetracene can also participate in the construction of solar cells. Its splitting speed is slower than that of pentacene, and singlet excitons are easily ionized directly at the molecular interface to reduce its photovoltaic conversion efficiency, but the energy level structure of tetracene is relatively ideal, its triplet exciton energy (1.2 eV) is close to the energy 1 eV corresponding to the maximum value of the SQ limit of single-junction solar cells. Jadhav inserted copper phthalocyanine (CuPC) into the structure of tetracene/C<sub>60</sub> to form a solar cell with three-layer film structure (Figure 14a) [95]. Tetracene absorbs light below 550 nm, singlets and triplets from tetracene diffuse through CuPC to the CuPC-C<sub>60</sub> interface (Figure 14b). BCP acts as an exciton and hole blocker. CuPC absorbs light below 700 nm and can provide extra triplet excitons in the long wavelength direction. The experimental results show that the photovoltaic device with the tetracene/CuPC/C<sub>60</sub> three-layer film structure exhibits higher external quantum efficiency and photovoltaic conversion performance than the double-layer structure. At the same time, the diffusion distance of triplet excitons is required to be longer.

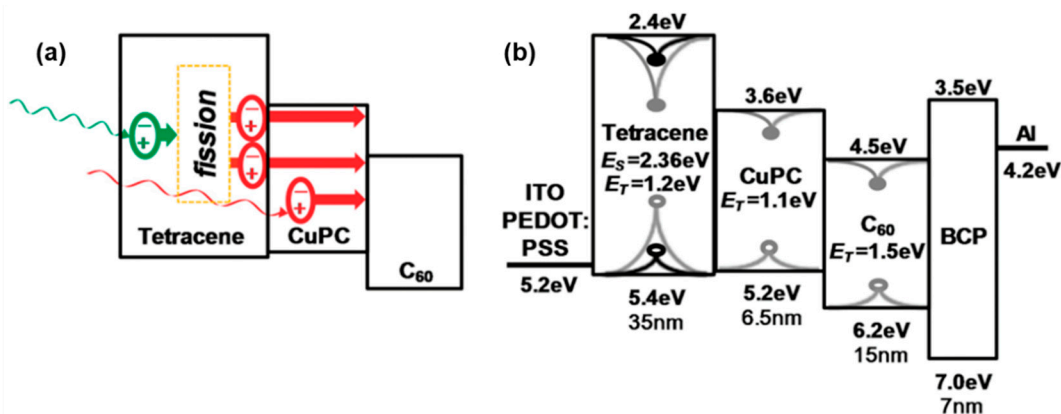


**Figure 14.** (a) Schematic of a photovoltaic exhibiting the SF process. (b) Complete structure of the photovoltaic cell. Reprinted with permission from Ref. [95]. Copyright 2011, American Chemical Society.

#### 4.2. Inorganic Solar Cells

Traditional inorganic solar cells are still the leader in photovoltaic devices, and the technology of single-junction silicon solar cells is increasingly perfected, with the highest conversion efficiency reaching 26.6% [96]. The SF process, as one of the ways of exciton multiplication, can theoretically further improve the photovoltaic conversion efficiency of single-junction solar cells. The main advantage of SF silicon solar cells is that it will make it easier to improve silicon solar cells that are already very efficient, which can greatly reduce the cost of solar cells and make them easier to fabricate and implement. Ehrler attempted to combine pentacene/PbSe heterojunction with undoped amorphous silicon to obtain a pentacene/PbSe/silicon three-layer SF sensitized inorganic photovoltaic device (Figure 15a). Visible range photons are absorbed by pentacene and split into pairs of low-energy triplet excitons. IR photons are absorbed in silicon and the thin PbSe layer. The total conversion rate reached 2% [97]. Subsequently, this group constructed an SF silicon-pentacene tandem solar cell device (Figure 15b), which showed an efficient photocurrent increase and an external quantum efficiency of over 100% for the main absorption peak of pentacene [98].

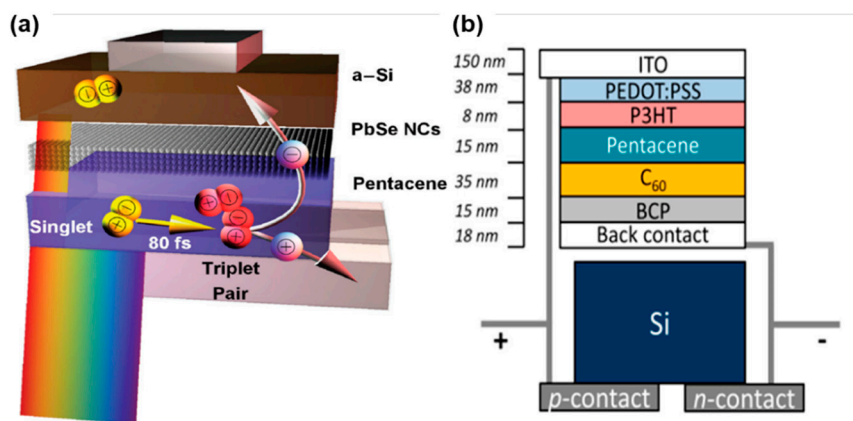


**Figure 15.** (a) Pentacene/PbSe/a-Si device structure and proposed working mechanism. (b) Device architecture of the parallel tandem cell. Reprinted with permission from Ref. [97] and Ref. [98]. Copyright 2012, AIP Publishing and 2017, American Chemical Society, respectively.

In 2020, Sundin studied the molecular SF dynamics of diphenylisobenzofuran derivatives on the surfaces of three different conduction band metal oxides, and found that both the semiconductor substrate and the environment around the molecules can influence the SF process [99]. When in a nonpolar environment, the SF process occurs when it attaches to  $ZrO_2$ , but when it is adsorbed on  $TiO_2$ , triplet states occur through charge recombination in the conduction band of  $TiO_2$ . In polar solvents, electron injection on  $TiO_2$  surface outperforms the SF process. When the molecule is attached to  $SnO_2$ , the SF process outperforms electron injection. Similarly, Ehrler calculated the efficiency potential of three technologically relevant SF silicon solar cell implementations (charge transfer, Dexter-type triplet energy transfer and Förster resonance energy transfer), and found the higher the efficiency of a silicon-based cell, the greater the efficiency gain of a singlet solar cell [100].

McQueen vapor-deposited tetracene on the surface of hydrogen-passivated crystalline silicon, and the silicon substrate maintained good passivation under the tetracene film. Pairs of triplet excitons generated in the SF layer diffuse to the silicon interface and transfer energy or charge, doubling the photocurrent (Figure 16a). Additionally, there are two exciton harvesting mechanisms being depicted at the organo-silicon interface: energy transfer (ET), and CT [101]. However, the external quantum efficiency indicates that the photocurrent contribution of the tetracene layer is very small, and the article does not explain the specific pathways of CT or ET at the heterojunction of tetracene and crystalline silicon. A double-heterojunction structure has been designed to overcome the effect of

exciton binding energy on batteries by placing a thin semiconducting layer between the SF material and the electron acceptor. With proper energy level arrangement, even in the presence of 0.5 eV exciton binding energy, an efficiency of 40.9% can be achieved, which is nearly 10% higher than that of a single heterojunction [102].

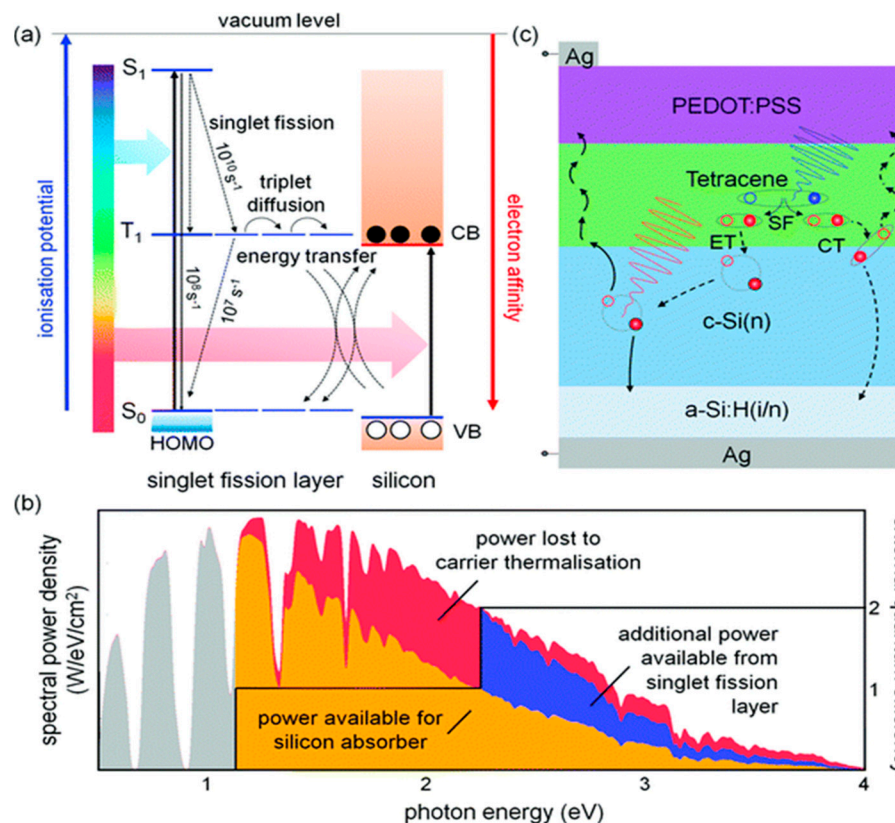


**Figure 16.** (a) Energy level diagram showing an organic SF layer situated as a selective absorber in a silicon-based solar cell. (b) Solar spectrum with shaded portions representing the approximate power available for electrical conversion in an ideal silicon solar cell (gold), the power lost to carrier thermalization (red) and sub-band gap transmission (grey), and the additional power made available by employing a matched SF layer (blue). The external quantum efficiency of the cell is drawn in black. (c) Solar cell structure utilized in this work (not to scale). Reprinted with permission from Ref. [101]. Copyright 2018, The Royal Society of Chemistry.

Baldo believed that the intermediate layer important if the triplet excitons were to be transferred to crystalline silicon without rapid recombination, so hafnium oxynitride, which could be deposited into an atomic layer on the surface of crystalline silicon, was selected as the intermediate layer. The power conversion efficiency of the silicon/hafnium oxynitride/tetracene photovoltaic cell with back contact reaches 5.1%, and the triplet exciton transfer rate reaches  $76 \pm 7\%$  [103].

### 5. Conclusions and Outlook

In recent years, the field of the SF process has made great progress, which is inseparable from the active exploration and research of scientists. In this paper, the development trend of SF materials in recent years and the in-depth exploration of the mechanism of the SF process were reviewed. Acenes and their derivatives are still the most powerful tools for scientists to study the SF process. Their molecular structure, arrangement and state of matter affect the degree of coupling between chromophores, which in turn affects the rate of the SF process and the triplet yield. There are also some emerging materials such as perylene diimide [35,38,104] and polymer [105–107], which have also been found to have a higher triplet yield and a longer triplet lifetime. In addition, this review also

introduced the application of the SF process in photovoltaic devices, among which there are currently realized cell structures, such as pentacene/ $C_{60}$ , pentacene/PbSe. Many attempts on this basis have been made, and there are also relatively new battery structures, such as double-heterojunction structure and cell structures combining pentacene and quantum dot.

With the research on SF materials, their applications are also developing at the same time, but relatively slow. At present, photovoltaic devices have been prepared with mature materials such as pentacene and tetracene, much progress has been made and a relatively good photovoltaic conversion efficiency has been achieved. The diversity and utility of new SF materials are the main drivers for future innovations in this field: First, developing more SF materials with energy-stable triplet states will expand our understanding of SF mechanisms, such as how to efficiently obtain triplet exciton energy, efficient triplet exciton dissociation, and transfer processes. Second, more unknown SF materials may surpass existing materials in improving the photovoltaic conversion efficiency of solar cells. Third, more novel materials may solve the long-term stability mismatch between SF molecules and conventional solar cell materials. Almost every published paper claims to study the SF process in order to improve the efficiency of solar energy conversion, but this is still a huge challenge in practice, and more studies will make efforts to this end.

**Author Contributions:** Conceptualization, J.L.; methodology, J.L.; investigation, H.C.; data curation, H.C.; writing—original draft preparation, J.L.; writing—review and editing, J.L.; visualization, S.L.; supervision, Z.Z.; project administration, Y.X.; funding acquisition, Y.X. All authors have read and agreed to the published version of the manuscript.

**Funding:** This research was funded by The National Nature Science Foundation of China (No.61975050, No.61675057) and The Nature Science Foundation of Hebei Province in China (F2021202055).

**Institutional Review Board Statement:** Not applicable.

**Informed Consent Statement:** Not applicable.

**Data Availability Statement:** The data that support the findings of this study are available from the corresponding author upon reasonable request.

**Conflicts of Interest:** The authors declare no conflict of interest.

## References

1. Wageh, S.; Raïssi, M.; Berthelot, T.; Laurent, M.; Rousseau, D.; Abusorrah, A.M.; Al-Hartomy, O.A.; Al-Ghamdi, A.A. Digital printing of a novel electrode for stable flexible organic solar cells with a power conversion efficiency of 8.5%. *Sci. Rep.* **2021**, *11*, 14212. [[CrossRef](#)] [[PubMed](#)]
2. Sharma, G.D.; Suthar, R.; Pestrikova, A.A.; Nikolaev, A.Y.; Chen, F.C.; Keshtov, M.L. Efficient Ternary Polymer solar cells based ternary active layer consisting of conjugated polymers and non-fullerene acceptors with power conversion efficiency approaching near to 15.5%. *Sol. Energy* **2021**, *216*, 217–224. [[CrossRef](#)]
3. An, Q.; Wang, J.; Gao, W.; Ma, X.; Hu, Z.; Gao, J.; Xu, C.; Hao, M.; Zhang, X.; Yang, C.; et al. Alloy-like ternary polymer solar cells with over 17.2% efficiency. *Sci. Bull.* **2020**, *65*, 538–545. [[CrossRef](#)]
4. Al-Ashouri, A.; Köhnen, E.; Li, B.; Magomedov, A.; Hempel, H.; Caprioglio, P.; Márquez, J.A.; Vilches, A.B.M.; Kasparavicius, E.; Smith, J.A.; et al. Monolithic perovskite/silicon tandem solar cell with >29% efficiency by enhanced hole extraction. *Science* **2020**, *370*, 1300–1309. [[CrossRef](#)]
5. Liu, X.; Zhang, C.; Pang, S.; Li, N.; Brabec, C.J.; Duan, C.; Huang, F.; Cao, Y. Ternary All-Polymer Solar Cells With 8.5% Power Conversion Efficiency and Excellent Thermal Stability. *Front. Chem.* **2020**, *8*, 302. [[CrossRef](#)]
6. Li, M.; Gao, K.; Wan, X.; Zhang, Q.; Kan, B.; Xia, R.; Liu, F.; Yang, X.; Feng, H.; Ni, W.; et al. Solution-processed organic tandem solar cells with power conversion efficiencies >12%. *Nat. Photonics* **2016**, *11*, 85–90. [[CrossRef](#)]
7. Chen, S.; Yao, H.; Hu, B.; Zhang, G.; Arunagiri, L.; Ma, L.K.; Huang, J.; Zhang, J.; Zhu, Z.; Bai, F.; et al. A Nonfullerene Semitransparent Tandem Organic Solar Cell with 10.5% Power Conversion Efficiency. *Adv. Energy Mater.* **2018**, *8*, 1800529. [[CrossRef](#)]
8. You, J.; Dou, L.; Yoshimura, K.; Kato, T.; Ohya, K.; Moriarty, T.; Emery, K.; Chen, C.-C.; Gao, J.; Li, G.; et al. A polymer tandem solar cell with 10.6% power conversion efficiency. *Nat. Commun.* **2013**, *4*, 1446. [[CrossRef](#)]
9. Shockley, W.; Queisser, H.J. Detailed Balance Limit of Efficiency of p-n Junction Solar Cells. *J. Appl. Phys.* **1961**, *32*, 510–519. [[CrossRef](#)]

10. Davis, N.J.L.K.; Böhm, M.L.; Tabachnyk, M.; Wisnivesky-Rocca-Rivarola, F.; Jellicoe, T.C.; Ducati, C.; Ehrler, B.; Greenham, N.C. Multiple-exciton generation in lead selenide nanorod solar cells with external quantum efficiencies exceeding 120%. *Nat. Commun.* **2015**, *6*, 8259. [[CrossRef](#)]
11. Hanna, M.C.; Nozik, A.J. Solar conversion efficiency of photovoltaic and photoelectrolysis cells with carrier multiplication absorbers. *J. Appl. Phys.* **2006**, *100*, 074510. [[CrossRef](#)]
12. Singh, S.; Jones, W.J.; Siebrand, W.; Stoicheff, B.P.; Schneider, W.G. Laser Generation of Excitons and Fluorescence in Anthracene Crystals. *J. Chem. Phys.* **1965**, *42*, 330–342. [[CrossRef](#)]
13. Merrifield, R.E.; Avakian, P.; Groff, R.P. Fission of singlet excitons into pairs of triplet excitons in tetracene crystals. *Chem. Phys. Lett.* **1969**, *3*, 386–388. [[CrossRef](#)]
14. Rademaker, H.; Hoff, A.J.; Grondelle, R.V.; Duysens, L.N. Carotenoid triplet yields in normal and deuterated Rhodospirillum rubrum. *Biochim. Biophys. Acta* **1980**, *592*, 240–257. [[CrossRef](#)]
15. Austin, R.H.; Baker, G.L.; Etemad, S.; Thompson, R. Magnetic field effects on triplet exciton fission and fusion in a polydiacetylene. *J. Chem. Phys.* **1989**, *90*, 6642–6646. [[CrossRef](#)]
16. Yarmus, L.; Rosenthal, J.; Chopp, M. EPR of triplet excitons in tetracene crystals: Spin polarization and the role of singlet exciton fission. *Chem. Phys. Lett.* **1972**, *16*, 477–481. [[CrossRef](#)]
17. Jundt, C.; Klein, G.; Sipp, B.; Moigne, J.L.; Joucla, M.; Villaeys, A.A. Exciton dynamics in pentacene thin films studied by pump-probe spectroscopy. *Chem. Phys. Lett.* **1995**, *24*, 84–88. [[CrossRef](#)]
18. Smith, M.B.; Michl, J. Singlet fission. *Chem. Rev.* **2010**, *110*, 6891–6936. [[CrossRef](#)]
19. Ito, S.; Nagami, T.; Nakano, M. Molecular design for efficient singlet fission. *J. Photochem. Photobiol. C* **2018**, *34*, 85–120. [[CrossRef](#)]
20. Korovina, N.V.; Pompetti, N.F.; Johnson, J.C. Lessons from intramolecular singlet fission with covalently bound chromophores. *J. Chem. Phys.* **2020**, *152*, 040904. [[CrossRef](#)]
21. Miyata, K.; Conrad-Burton, F.S.; Geyer, F.L.; Zhu, X.Y. Triplet Pair States in Singlet Fission. *Chem. Rev.* **2019**, *119*, 4261–4292. [[CrossRef](#)] [[PubMed](#)]
22. Chan, W.-L.; Berkelbach, T.C.; Provorse, M.R.; Monahan, N.R.; Tritsch, J.R.; Hybertsen, M.S.; Reichman, D.R.; Gao, J.; Zhu, X.-Y. The Quantum Coherent Mechanism for Singlet Fission: Experiment and Theory. *Acc. Chem. Res.* **2013**, *46*, 1321–1329. [[CrossRef](#)] [[PubMed](#)]
23. Felter, K.M.; Grozema, F.C. Singlet Fission in Crystalline Organic Materials: Recent Insights and Future Directions. *J. Phys. Chem. Lett.* **2019**, *10*, 7208–7214. [[CrossRef](#)] [[PubMed](#)]
24. Xia, J.; Sanders, S.N.; Cheng, W.; Low, J.Z.; Liu, J.; Campos, L.M.; Sun, T. Singlet Fission: Progress and Prospects in Solar Cells. *Adv. Mater.* **2017**, *29*, 1601652. [[CrossRef](#)]
25. Smith, M.B.; Michl, J. Recent Advances in Singlet Fission. *Annu. Rev. Phys. Chem.* **2013**, *64*, 361–386. [[CrossRef](#)]
26. Burdett, J.J.; Bardeen, C.J. The Dynamics of Singlet Fission in Crystalline Tetracene and Covalent Analogs. *Acc. Chem. Res.* **2013**, *46*, 1312–1320. [[CrossRef](#)]
27. Monahan, N.; Zhu, X.Y. Charge transfer-mediated singlet fission. *Annu. Rev. Phys. Chem.* **2015**, *66*, 601–618. [[CrossRef](#)]
28. Parker, S.M.; Seideman, T.; Ratner, M.A.; Shiozaki, T. Model Hamiltonian Analysis of Singlet Fission from First Principles. *J. Phys. Chem. C* **2014**, *118*, 12700–12705. [[CrossRef](#)]
29. Japahuge, A.; Zeng, T. Theoretical Studies of Singlet Fission: Searching for Materials and Exploring Mechanisms. *Chempluschem* **2018**, *83*, 146–182. [[CrossRef](#)]
30. Rao, A.; Friend, R.H. Harnessing singlet exciton fission to break the Shockley–Queisser limit. *Nat. Rev. Mater.* **2017**, *2*, 17063. [[CrossRef](#)]
31. Ullrich, T.; Munz, D.; Guldi, D.M. Unconventional singlet fission materials. *Chem. Soc. Rev.* **2021**, *50*, 3485–3518. [[CrossRef](#)] [[PubMed](#)]
32. Wilson, M.W.; Rao, A.; Johnson, K.; Gelinas, S.; di Pietro, R.; Clark, J.; Friend, R.H. Temperature-Independent Singlet Exciton Fission in Tetracene. *J. Am. Chem. Soc.* **2013**, *135*, 16680–16688. [[CrossRef](#)] [[PubMed](#)]
33. Tayebjee, M.J.Y.; Gray-Weale, A.A.; Schmidt, T.W. Thermodynamic Limit of Exciton Fission Solar Cell Efficiency. *J. Phys. Chem. Lett.* **2012**, *3*, 2749–2754. [[CrossRef](#)]
34. Stern, H.L.; Cheminal, A.; Yost, S.R.; Broch, K.; Bayliss, S.L.; Chen, K.; Tabachnyk, M.; Thorley, K.; Greenham, N.; Hodgkiss, J.M.; et al. Vibronically coherent ultrafast triplet-pair formation and subsequent thermally activated dissociation control efficient endothermic singlet fission. *Nat. Chem.* **2017**, *9*, 1205–1212. [[CrossRef](#)] [[PubMed](#)]
35. Le, A.K.; Bender, J.A.; Arias, D.H.; Cotton, D.E.; Johnson, J.C.; Roberts, S.T. Singlet Fission Involves an Interplay between Energetic Driving Force and Electronic Coupling in Perylenediimide Films. *J. Am. Chem. Soc.* **2018**, *140*, 814–826. [[CrossRef](#)] [[PubMed](#)]
36. Yong, C.K.; Musser, A.J.; Bayliss, S.L.; Lukman, S.; Tamura, H.; Bubnova, O.; Hallani, R.K.; Meneau, A.; Resel, R.; Maruyama, M.; et al. The Entangled Triplet Pair State in Acene and Heteroacene Materials. *Nat. Commun.* **2017**, *8*, 15953. [[CrossRef](#)] [[PubMed](#)]
37. Pensack, R.D.; Tilley, A.J.; Grieco, C.; Purdum, G.E.; Ostroumov, E.E.; Granger, D.B.; Oblinsky, D.G.; Dean, J.C.; Doucette, G.S.; Asbury, J.B.; et al. Striking the right balance of intermolecular coupling for high-efficiency singlet fission. *Chem. Sci.* **2018**, *9*, 6240–6259. [[CrossRef](#)]
38. Margulies, E.A.; Miller, C.E.; Wu, Y.; Ma, L.; Schatz, G.C.; Young, R.M.; Wasielewski, M.R. Enabling singlet fission by controlling intramolecular charge transfer in pi-stacked covalent terrylenediimide dimers. *Nat. Chem.* **2016**, *8*, 1120–1125. [[CrossRef](#)]

39. Monahan, N.R.; Sun, D.; Tamura, H.; Williams, K.W.; Xu, B.; Zhong, Y.; Kumar, B.; Nuckolls, C.; Harutyunyan, A.R.; Chen, G.; et al. Dynamics of the triplet-pair state reveals the likely coexistence of coherent and incoherent singlet fission in crystalline hexacene. *Nat. Chem.* **2017**, *9*, 341–346. [[CrossRef](#)]
40. Yago, T.; Ishikawa, K.; Katoh, R.; Wakasa, M. Magnetic Field Effects on Triplet Pair Generated by Singlet Fission in an Organic Crystal: Application of Radical Pair Model to Triplet Pair. *J. Phys. Chem. C* **2016**, *120*, 27858–27870. [[CrossRef](#)]
41. Piland, G.B.; Bardeen, C.J. How Morphology Affects Singlet Fission in Crystalline Tetracene. *J. Phys. Chem. Lett.* **2015**, *6*, 1841–1846. [[CrossRef](#)]
42. Ryerson, J.L.; Schrauben, J.N.; Ferguson, A.J.; Sahoo, S.C.; Naumov, P.; Havlas, Z.; Michl, J.; Nozik, A.J.; Johnson, J.C. Two Thin Film Polymorphs of the Singlet Fission Compound 1,3-Diphenylisobenzofuran. *J. Phys. Chem. C* **2014**, *118*, 12121–12132. [[CrossRef](#)]
43. Roberts, S.T.; McAnally, R.E.; Mastron, J.N.; Webber, D.H.; Whited, M.T.; Brutchey, R.L.; Thompson, M.E.; Bradforth, S.E. Efficient Singlet Fission Discovered in a Disordered Acene Film. *J. Am. Chem. Soc.* **2012**, *134*, 6388–6400. [[CrossRef](#)] [[PubMed](#)]
44. Wilson, M.W.B.; Rao, A.; Clark, J.; Kumar, R.S.S.; Brida, D.; Cerullo, G.; Friend, R.H. Ultrafast Dynamics of Exciton Fission in Polycrystalline Pentacene. *J. Am. Chem. Soc.* **2011**, *133*, 11830–11833. [[CrossRef](#)] [[PubMed](#)]
45. Busby, E.; Xia, J.; Low, J.Z.; Wu, Q.; Hoy, J.; Campos, L.M.; Sfeir, M.Y. Fast Singlet Exciton Decay in Push-Pull Molecules Containing Oxidized Thiophenes. *J. Phys. Chem. B* **2015**, *119*, 7644–7650. [[CrossRef](#)]
46. Young, R.M.; Wasielewski, M.R. Mixed Electronic States in Molecular Dimers: Connecting Singlet Fission, Excimer Formation, and Symmetry-Breaking Charge Transfer. *Acc. Chem. Res.* **2020**, *53*, 1957–1968. [[CrossRef](#)]
47. Busby, E.; Berkelbach, T.C.; Kumar, B.; Chernikov, A.; Zhong, Y.; Hlaing, H.; Zhu, X.-Y.; Heinz, T.F.; Hybertsen, M.S.; Sfeir, M.Y.; et al. Multiphonon Relaxation Slows Singlet Fission in Crystalline Hexacene. *J. Am. Chem. Soc.* **2014**, *136*, 10654–10660. [[CrossRef](#)]
48. Zhou, Z.; Ma, L.; Guo, D.; Zhao, X.; Wang, C.; Lin, D.; Zhang, F.; Zhang, J.; Nie, Z. Ultrafast Dynamics of Long-Lived Bound Triplet Pair Generated by Singlet Fission in 6,13-Bis(triisopropylsilylethynyl) Pentacene. *J. Phys. Chem. C* **2020**, *124*, 14503–14509. [[CrossRef](#)]
49. Zhang, Z.; Ni, W.; Ma, L.; Sun, L.; Gurzadyan, G.G. Enhancement of Singlet Fission Yield by Hindering Excimer Formation in Perylene Film. *J. Phys. Chem. C* **2021**, *126*, 396–403. [[CrossRef](#)]
50. Berera, R.; van Grondelle, R.; Kennis, J.T. Ultrafast transient absorption spectroscopy: Principles and application to photosynthetic systems. *Photosynth. Res.* **2009**, *101*, 105–118. [[CrossRef](#)]
51. Eaton, S.W.; Shoer, L.E.; Karlen, S.D.; Dyar, S.M.; Margulies, E.A.; Veldkamp, B.S.; Ramanan, C.; Hartzler, D.A.; Savikhin, S.; Marks, T.J.; et al. Singlet Exciton Fission in Polycrystalline Thin Films of a Slip-stacked Perylenediimide. *J. Am. Chem. Soc.* **2013**, *135*, 14701–14712. [[CrossRef](#)] [[PubMed](#)]
52. Dvořák, M.; Prasad, S.K.K.; Dover, C.B.; Forest, C.R.; Kaleem, A.; MacQueen, R.W.; Petty, A.J.; Forecast, R.; Beves, J.E.; Anthony, J.E.; et al. Singlet Fission in Concentrated TIPS-Pentacene Solutions: The Role of Excimers and Aggregates. *J. Am. Chem. Soc.* **2021**, *143*, 13749–13758. [[CrossRef](#)] [[PubMed](#)]
53. Liu, H.; Wang, R.; Shen, L.; Xu, Y.; Xiao, M.; Zhang, C.; Li, X. A Covalently Linked Tetracene Trimer: Synthesis and Singlet Exciton Fission Property. *Org. Lett.* **2017**, *19*, 580–583. [[CrossRef](#)]
54. Lukman, S.; Richter, J.M.; Yang, L.; Hu, P.; Wu, J.; Greenham, N.C.; Musser, A.J. Efficient Singlet Fission and Triplet-Pair Emission in a Family of Zethrene Diradicaloids. *J. Am. Chem. Soc.* **2017**, *139*, 18376–18385. [[CrossRef](#)]
55. Nandi, A.; Manna, B.; Ghosh, R. Singlet Fission Dynamics in the 5,12-Bis(phenylethynyl)tetracene Thin Film. *J. Phys. Chem. C* **2021**, *125*, 2583–2591. [[CrossRef](#)]
56. Chan, W.L.; Ligges, M.; Zhu, X.Y. The Energy Barrier in Singlet Fission can be Overcome through Coherent Coupling and Entropic Gain. *Nat. Chem.* **2012**, *4*, 840–845. [[CrossRef](#)] [[PubMed](#)]
57. Walker, B.J.; Musser, A.J.; Beljonne, D.; Friend, R.H. Singlet exciton fission in solution. *Nat. Chem.* **2013**, *5*, 1019–1024. [[CrossRef](#)]
58. Lee, J.; Bruzek, M.J.; Thompson, N.J.; Sfeir, M.Y.; Anthony, J.E.; Baldo, M.A. Singlet Exciton Fission in a Hexacene Derivative. *Adv. Mater.* **2013**, *25*, 1445–1448. [[CrossRef](#)]
59. Watanabe, M.; Chang, Y.J.; Liu, S.W.; Chao, T.H.; Goto, K.; Islam, M.M.; Yuan, C.H.; Tao, Y.T.; Shinmyozu, T.; Chow, T.J. The Synthesis, Crystal Structure and Charge-Transport Properties of Hexacene. *Nat. Chem.* **2012**, *4*, 574–578. [[CrossRef](#)]
60. Johnson, J.C.; Nozik, A.J.; Michl, J. High Triplet Yield from Singlet Fission in a Thin Film of 1,3-Diphenylisobenzofuran. *J. Am. Chem. Soc.* **2010**, *132*, 16302–16303. [[CrossRef](#)]
61. Marciniak, H.; Pugliesi, I.; Nickel, B.; Lochbrunner, S. Ultrafast singlet and triplet dynamics in microcrystalline pentacene films. *Phys. Rev. B* **2009**, *79*, 235318. [[CrossRef](#)]
62. Marciniak, H.; Fiebig, M.; Huth, M.; Schiefer, S.; Nickel, B.; Selmaier, F.; Lochbrunner, S. Ultrafast exciton relaxation in microcrystalline pentacene films. *Phys. Rev. Lett.* **2007**, *99*, 176402. [[CrossRef](#)] [[PubMed](#)]
63. Thorsmolle, V.K.; Averitt, R.D.; Demsar, J.; Smith, D.L.; Tretiak, S.; Martin, R.L.; Chi, X.; Crone, B.K.; Ramirez, A.P.; Taylor, A.J. Morphology effectively controls singlet-triplet exciton relaxation and charge transport in organic semiconductors. *Phys. Rev. Lett.* **2009**, *102*, 017401. [[CrossRef](#)] [[PubMed](#)]
64. Korovina, N.V.; Das, S.; Nett, Z.; Feng, X.; Joy, J.; Haiges, R.; Krylov, A.I.; Bradforth, S.E.; Thompson, M.E. Singlet Fission in a Covalently Linked Cofacial Alkynyltetracene Dimer. *J. Am. Chem. Soc.* **2016**, *138*, 617–627. [[CrossRef](#)]
65. Feng, X.; Krylov, A.I. On couplings and excimers: Lessons from studies of singlet fission in covalently linked tetracene dimers. *Phys. Chem. Chem. Phys.* **2016**, *18*, 7751–7761. [[CrossRef](#)] [[PubMed](#)]

66. Feng, X.; Casanova, D.; Krylov, A.I. Intra- and Intermolecular Singlet Fission in Covalently Linked Dimers. *J. Phys. Chem. C* **2016**, *120*, 19070–19077. [[CrossRef](#)]
67. Jones, A.C.; Kearns, N.M.; Ho, J.J.; Flach, J.T.; Zanni, M.T. Impact of non-equilibrium molecular packings on singlet fission in microcrystals observed using 2D white-light microscopy. *Nat. Chem.* **2020**, *12*, 40–47. [[CrossRef](#)]
68. Ribson, R.D.; Choi, G.; Hadt, R.G.; Agapie, T. Controlling Singlet Fission with Coordination Chemistry-Induced Assembly of Dipyridyl Pyrrole Bipentacenes. *ACS Cent. Sci.* **2020**, *6*, 2088–2096. [[CrossRef](#)]
69. Munson, K.T.; Gan, J.; Grieco, C.; Doucette, G.S.; Anthony, J.E.; Asbury, J.B. Ultrafast Triplet Pair Separation and Triplet Trapping following Singlet Fission in Amorphous Pentacene Films. *J. Phys. Chem. C* **2020**, *124*, 23567–23578. [[CrossRef](#)]
70. Luo, X.; Han, Y.; Chen, Z.; Li, Y.; Liang, G.; Liu, X.; Ding, T.; Nie, C.; Wang, M.; Castellano, F.N.; et al. Mechanisms of triplet energy transfer across the inorganic nanocrystal/organic molecule interface. *Nat. Commun.* **2020**, *11*, 28. [[CrossRef](#)]
71. Yan, X.; Liu, H.; Wang, X.; Liu, S.; Zhao, D.; Tang, Z.; Zhou, J.; Li, X. Singlet Fission in Self-assembled Amphiphathic Tetracene Nanoparticles: Probing the Role of Charge-transfer State. *J. Photochem. Photobiol. A* **2020**, *397*, 112597. [[CrossRef](#)]
72. Tang, Z.; Zhou, S.; Wang, X.; Liu, H.; Yan, X.; Liu, S.; Lu, X.; Li, X. Enhancing the intermolecular singlet fission efficiency by controlling the self-assembly of amphiphathic tetracene derivatives in aqueous solution. *J. Mater. Chem. C* **2019**, *7*, 11090–11098. [[CrossRef](#)]
73. Wilson, M.W.B.; Rao, A.; Ehrler, B.; Friend, R.H. Singlet Exciton Fission in Polycrystalline Pentacene: From Photophysics toward Devices. *Acc. Chem. Res.* **2013**, *46*, 1330–1338. [[CrossRef](#)] [[PubMed](#)]
74. Sheraw, C.D.; Jackson, T.N.; Eaton, D.L.; Anthony, J.E. Functionalized Pentacene Active Layer Organic Thin-Film Transistors. *Adv. Mater.* **2003**, *15*, 2009–2011. [[CrossRef](#)]
75. Grieco, C.; Doucette, G.S.; Munson, K.T.; Swartzfager, J.R.; Munro, J.M.; Anthony, J.E.; Dabo, I.; Asbury, J.B. Vibrational probe of the origin of singlet exciton fission in TIPS-pentacene solutions. *J. Chem. Phys.* **2019**, *151*, 154701. [[CrossRef](#)]
76. Cui, M.; Jiang, Y.; Zhang, B.; Song, D.; Yuan, M.; Qin, C.; Liu, Y. Multiexciton state of singlet fission in triisopropylsilylethynyl-pentacene. *Microw. Opt. Technol. Lett.* **2021**, *63*, 1399–1405. [[CrossRef](#)]
77. Herz, J.; Backup, T.; Paulus, F.; Engelhart, J.; Bunz, U.H.; Motzkus, M. Acceleration of Singlet Fission in an Aza-Derivative of TIPS-Pentacene. *J. Phys. Chem. Lett.* **2014**, *5*, 2425–2430. [[CrossRef](#)]
78. Sanders, S.N.; Kumarasamy, E.; Pun, A.B.; Trinh, M.T.; Choi, B.; Xia, J.; Taffet, E.J.; Low, J.Z.; Miller, J.R.; Roy, X.; et al. Quantitative Intramolecular Singlet Fission in Bipentacenes. *J. Am. Chem. Soc.* **2015**, *137*, 8965–8972. [[CrossRef](#)]
79. Paul, S.; Karunakaran, V. Excimer Formation Inhibits the Intramolecular Singlet Fission Dynamics: Systematic Tilting of Pentacene Dimers by Linking Positions. *J. Phys. Chem. B* **2022**, *126*, 1054–1062. [[CrossRef](#)]
80. Alagna, N.; Perez Lustres, J.L.; Wollscheid, N.; Luo, Q.; Han, J.; Dreuw, A.; Geyer, F.L.; Brosius, V.; Bunz, U.H.F.; Backup, T.; et al. Singlet Fission in Tetraaza-TIPS-Pentacene Oligomers: From fs Excitation to ns Triplet Decay via the Biexcitonic State. *J. Phys. Chem. B* **2019**, *123*, 10780–10793. [[CrossRef](#)]
81. Vallett, P.J.; Snyder, J.L.; Damrauer, N.H. Tunable electronic coupling and driving force in structurally well-defined tetracene dimers for molecular singlet fission: A computational exploration using density functional theory. *J. Phys. Chem. A* **2013**, *117*, 10824–10838. [[CrossRef](#)]
82. Zirzmeier, J.; Lehnher, D.; Coto, P.B.; Chernick, E.T.; Casillas, R.; Basel, B.S.; Thoss, M.; Tykwinski, R.R.; Guldi, D.M. Singlet fission in pentacene dimers. *Proc. Natl. Acad. Sci. USA* **2015**, *112*, 5325–5330. [[CrossRef](#)] [[PubMed](#)]
83. Paul, S.; Govind, C.; Karunakaran, V. Planarity and Length of the Bridge Control Rate and Efficiency of Intramolecular Singlet Fission in Pentacene Dimers. *J. Phys. Chem. B* **2021**, *125*, 231–239. [[CrossRef](#)]
84. Sanders, S.N.; Kumarasamy, E.; Pun, A.B.; Steigerwald, M.L.; Sfeir, M.Y.; Campos, L.M. Intramolecular Singlet Fission in Oligoacene Heterodimers. *Angew. Chem., Int. Ed.* **2016**, *55*, 3373–3377. [[CrossRef](#)]
85. Liu, H.; Wang, Z.; Wang, X.; Shen, L.; Zhang, C.; Xiao, M.; Li, X. Singlet exciton fission in a linear tetracene tetramer. *J. Mater. Chem. C* **2018**, *6*, 3245–3253. [[CrossRef](#)]
86. Kuroda, K.; Yazaki, K.; Tanaka, Y.; Akita, M.; Sakai, H.; Hasobe, T.; Tkachenko, N.V.; Yoshizawa, M. A Pentacene-based Nanotube Displaying Enriched Electrochemical and Photochemical Activities. *Angew. Chem. Int. Ed.* **2019**, *58*, 1115–1119. [[CrossRef](#)]
87. Huang, H.; He, G.; Xu, K.; Wu, Q.; Wu, D.; Sfeir, M.Y.; Xia, J. Achieving Long-Lived Triplet States in Intramolecular SF Films through Molecular Engineering. *Chem* **2019**, *5*, 2405–2417. [[CrossRef](#)]
88. Lee, J.; Jadhav, P.; Baldo, M.A. High efficiency organic multilayer photodetectors based on singlet exciton fission. *Appl. Phys. Lett.* **2009**, *95*, 033301. [[CrossRef](#)]
89. Congreve, D.N.; Lee, J.; Thompson, N.J.; Hontz, E.; Yost, S.R.; Reuswig, P.D.; Bahlke, M.E.; Reineke, S.; Van Voorhis, T.; Baldo, M.A. External Quantum Efficiency Above 100% in a Singlet-Exciton-Fission-Based Organic Photovoltaic Cell. *Science* **2013**, *340*, 334–337. [[CrossRef](#)]
90. Thompson, N.J.; Congreve, D.N.; Goldberg, D.; Menon, V.M.; Baldo, M.A. Slow light enhanced singlet exciton fission solar cells with a 126% yield of electrons per photon. *Appl. Phys. Lett.* **2013**, *103*, 263302. [[CrossRef](#)]
91. Rao, A.; Wilson, M.W.B.; Hodgkiss, J.M.; Albert-Seifried, S.; Bäessler, H.; Friend, R.H. Exciton Fission and Charge Generation via Triplet Excitons in Pentacene/C60Bilayers. *J. Am. Chem. Soc.* **2010**, *132*, 12698–12703. [[CrossRef](#)] [[PubMed](#)]
92. Chan, W.-L.; Ligges, M.; Jailaubekov, A.; Kaake, L.; Miaja-Avila, L.; Zhu, X.-Y. Observing the Multiexciton State in Singlet Fission and Ensuing Ultrafast Multielectron Transfer. *Science* **2011**, *334*, 1541–1545. [[CrossRef](#)] [[PubMed](#)]

93. Jadhav, P.J.; Brown, P.R.; Thompson, N.; Wunsch, B.; Mohanty, A.; Yost, S.R.; Hontz, E.; Van Voorhis, T.; Bawendi, M.G.; Bulović, V.; et al. Triplet Exciton Dissociation in Singlet Exciton Fission Photovoltaics. *Adv. Mater.* **2012**, *24*, 6169–6174. [[CrossRef](#)] [[PubMed](#)]
94. Yang, L.; Tabachnyk, M.; Bayliss, S.L.; Böhm, M.L.; Broch, K.; Greenham, N.C.; Friend, R.H.; Ehrler, B. Solution-Processable Singlet Fission Photovoltaic Devices. *Nano Lett.* **2014**, *15*, 354–358. [[CrossRef](#)] [[PubMed](#)]
95. Jadhav, P.J.; Mohanty, A.; Sussman, J.; Lee, J.; Baldo, M.A. Singlet Exciton Fission in Nanostructured Organic Solar Cells. *Nano Lett.* **2011**, *11*, 1495–1498. [[CrossRef](#)] [[PubMed](#)]
96. Editorial A decade of perovskite photovoltaics. *Nat. Energy* **2019**, *4*, 1. [[CrossRef](#)]
97. Ehrler, B.; Musselman, K.P.; Böhm, M.L.; Friend, R.H.; Greenham, N.C. Hybrid pentacene/a-silicon solar cells utilizing multiple carrier generation via singlet exciton fission. *Appl. Phys. Lett.* **2012**, *101*, 153507. [[CrossRef](#)]
98. Pazos-Outón, L.M.; Lee, J.M.; Futscher, M.H.; Kirch, A.; Tabachnyk, M.; Friend, R.H.; Ehrler, B. A Silicon–Singlet Fission Tandem Solar Cell Exceeding 100% External Quantum Efficiency with High Spectral Stability. *ACS Energy Lett.* **2017**, *2*, 476–480. [[CrossRef](#)]
99. Sundin, E.; Ringström, R.; Johansson, F.; Küçüköz, B.; Ekebergh, A.; Gray, V.; Albinsson, B.; Mårtensson, J.; Abrahamsson, M. Singlet Fission and Electron Injection from the Triplet Excited State in Diphenylisobenzofuran–Semiconductor Assemblies: Effects of Solvent Polarity and Driving Force. *J. Phys. Chem. C* **2020**, *124*, 20794–20805. [[CrossRef](#)]
100. Daiber, B.; van den Hoven, K.; Futscher, M.H.; Ehrler, B. Realistic Efficiency Limits for Singlet-Fission Silicon Solar Cells. *ACS Energy Lett.* **2021**, *6*, 2800–2808. [[CrossRef](#)]
101. MacQueen, R.W.; Liebhaber, M.; Niederhausen, J.; Mews, M.; Gersmann, C.; Jäckle, S.; Jäger, K.; Tayebjee, M.J.Y.; Schmidt, T.W.; Rech, B.; et al. Crystalline silicon solar cells with tetracene interlayers: The path to silicon-singlet fission heterojunction devices. *Mater. Horiz.* **2018**, *5*, 1065–1075. [[CrossRef](#)]
102. Cheung, J.C.F.; Kaake, L.G. Detailed balance analysis of advanced geometries for singlet fission solar cells. *Appl. Phys. Lett.* **2021**, *119*, 013301. [[CrossRef](#)]
103. Einzinger, M.; Wu, T.; Kompalla, J.F.; Smith, H.L.; Perkinson, C.F.; Nienhaus, L.; Wieghold, S.; Congreve, D.N.; Kahn, A.; Bawendi, M.G.; et al. Sensitization of silicon by singlet exciton fission in tetracene. *Nature* **2019**, *571*, 90–94. [[CrossRef](#)] [[PubMed](#)]
104. Carlotti, B.; Madu, I.K.; Kim, H.; Cai, Z.; Jiang, H.; Muthike, A.K.; Yu, L.; Zimmerman, P.M.; Goodson, T., 3rd. Activating intramolecular singlet exciton fission by altering pi-bridge flexibility in perylene diimide trimers for organic solar cells. *Chem. Sci.* **2020**, *11*, 8757–8770. [[CrossRef](#)] [[PubMed](#)]
105. Korovina, N.V.; Chang, C.H.; Johnson, J.C. Spatial separation of triplet excitons drives endothermic singlet fission. *Nat. Chem.* **2020**, *12*, 391–398. [[CrossRef](#)]
106. Hu, J.; Xu, K.; Shen, L.; Wu, Q.; He, G.; Wang, J.Y.; Pei, J.; Xia, J.; Sfeir, M.Y. New insights into the design of conjugated polymers for intramolecular singlet fission. *Nat. Commun.* **2018**, *9*, 2999. [[CrossRef](#)]
107. Wang, L.; Cai, W.; Sun, J.; Wu, Y.; Zhang, B.; Tian, X.; Guo, S.; Liang, W.; Fu, H.; Yao, J. H-Type-like Aggregation-Accelerated Singlet Fission Process in Dipyrrolonaphthyridinedione Thin Film: The Role of Charge Transfer/Excimer Mixed Intermediate State. *J. Phys. Chem. Lett.* **2021**, *12*, 12276–12282. [[CrossRef](#)]